

## Response to Comments of Editor

(comments in *italics*)

**Manuscript number:** acp-2021-119

**Title:** Impacts of aerosol-photolysis interaction and aerosol-radiation feedback on surface-layer ozone in North China during a multi-pollutant air pollution episode

*Reviewer #2 said that the paper suffers from analyzing a small region over a few days, making it hard to draw broader conclusions. Reviewer #2 further said that the paper should either 1) make clear how the paper is methodologically novel or 2) analyze a longer period(s) so that we understand better how general the results are. I understand that the focus is on severely polluted conditions, and so you wouldn't simulate a full year, for example.*

*I agree with Reviewer #2's assessment. In response, no case is made for methodological novelty. Two additional short episodes are added to the paper, for which apparently similar conclusions are reached. But those two episodes are added as an after-thought - they appear only in a separate Discussion section, with all relevant figures in the supporting information. No case is made for why these two extra episodes are less important to justify keeping the focus on the first episode.*

*I do not think it would be worthwhile to send the current version to the same referees in its current form. Rather, I think the authors should rewrite the paper to talk about the analysis of 3 episodes throughout, from the introduction through to conclusions - unless the authors can justify the main focus on one episode and secondary focus on the 2 others. You are free to respond as you'd like, but that is my strong recommendation.*

*Apart from that, I felt that the authors gave good responses to many of the individual points from the 2 referees, but often did not go far enough to change the paper itself to address those concerns. For example, Figure R2 seems to me to show that the model is a factor of two too low in AOD.*

*If you would like to resubmit to ACP, please make substantial revisions to the paper to incorporate the 3 episodes throughout the paper, and prepare an improved response to reviewers that more fully shows how the paper is improved as a results of responding to comments.*

### Response:

Thanks for the Editor's valuable comments to this manuscript. We totally agree with your helpful suggestions, and we have made substantial revisions in the final revised paper.

Three complex air pollution episodes (Episode1: 28 July-3 August 2014, Episode2: 8-13 July 2015, Episode3: 5-11 June 2016) are selected and analyzed throughout the whole revised manuscript, and the general conclusion can be summarized that API (aerosol-photolysis interaction) is the dominant factor for O<sub>3</sub> reduction related to aerosol-radiation interactions during all the simulated episodes.

According to the Editor's comments, all the responses to the two reviewers are rewritten. The new updated responses and the final revised paper can clearly show how the manuscript is improved.

**Response to “Figure R2 seems to me to show that the model is a factor of two too low in AOD”**

Thank you for your comments. Previous studies find that MODIS retrievals can overestimate AOD in NCP during polluted events when comparing with observations collected from AERONET (Gao et al., 2015; Li et al., 2016). Therefore, comparisons between simulated AOD and AERONET observations are conducted in this work. The revised Fig. R2 shows the correlation between observed and simulated AOD at 550 nm in Beijing. In the WRF-Chem model, the AOD at 550 nm are calculated by using the values at 400 and 600 nm according to the Angstrom exponent. Analyzing Fig. R2, the model can reproduce the observed AOD with R of 0.7 and NMB of 7.9%. (Page 8, Line 190-193)

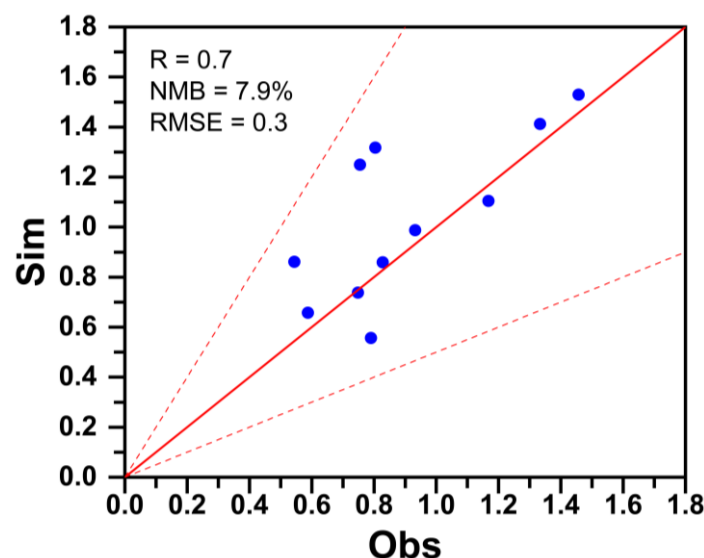


**Figure R2.** Comparison of observed and simulated AOD at 550 nm in Beijing (39.98°N, 116.38°E). The observed AOD during the three episodes are collected from AERONET.

**Reference:**

- Gao, Y., Zhang, M., Liu, Z., Wang, L., Wang, P., Xia, X., Tao, M., and Zhu, L.: Modeling the feedback between aerosol and meteorological variables in the atmospheric boundary layer during a severe fog–haze event over the North China Plain, *Atmos. Chem. Phys.*, 15, 4279–4295, doi:10.5194/acp-15-4279-2015, 2015.
- Li, K., Liao, H., Zhu, J., and Moch, J. M.: Implications of RCP emissions on future PM<sub>2.5</sub> air quality and direct radiative forcing over China, *J. Geophys. Res. Atmos.*, 121, 12,985–13,008, doi:10.1002/2016JD025623, 2016.

**Thank you very much for your comments and suggestions.**

# Response to Comments of Reviewer #1

(comments in *italics*)

**Manuscript number:** acp-2021-119

**Title:** Impacts of aerosol-photolysis interaction and aerosol-radiation feedback on surface-layer ozone in North China during a multi-pollutant air pollution episode

*Yang et al. examined the impacts of aerosols on surface ozone through the two well-known pathways, i.e., aerosol-photolysis interaction and aerosol-radiation feedback. The novelty of this study is its focus on the polluted episodes with elevated both PM<sub>2.5</sub> and ozone levels over North China. They also quantified the chemical and physical processes that drive the aerosol-radiation interactions.*

*Overall, this is a timely study and it clearly demonstrates the impacts of aerosols on ozone pollution. The structure of this manuscript is easy to follow. Although some of the manuscript needs further clarification, the results are generally convincing. As such, I think it is publishable after the following issues are addressed.*

## **Response:**

Thanks to the reviewer for the valuable comments and suggestions which are very helpful for us to improve our manuscript. We have revised the manuscript carefully, as described in our point-to-point responses to the comments.

## **Specific Comments:**

1. *In Abstract: ozone changes refer to MDA8 ozone or daytime ozone?*

## **Response:**

The ozone changes in abstract mean daytime ozone. According to the reviewer's comments, we have added this information in the revised manuscript. (Page 2, Line 34)

2. *Line 177: a correlation coefficient of 0.66 reads like not high!*

## **Response:**

According to the comments of Reviewer#2, another two complex air pollution episodes (8-13 July 2015 (Episode2) and 5-11 June 2016 (Episode3)) in this region are selected to conduct simulations for generating general conclusions.

Thanks for your suggestion, we have changed this sentence in the revised manuscript as follows: "As shown in Fig. 2, the temporal variations of observed PM<sub>2.5</sub> can be well performed by the model with correlation coefficients (R) of 0.66, 0.56 and 0.73 and normalized mean bias (NMB) of -19.2%, -3.9% and 30.4% during Episode1, Episode2 and Episode3, respectively." (Page 7-8, Line 183-186)

3. *Lines 179-181: the oxidation of SO<sub>2</sub> by NO<sub>2</sub> in aqueous aerosols is important for summertime?*

## **Response:**

This sentence has been deleted in the revised manuscript.

4. *Lines 248-251: this statement looks reasonable here, but in the later text the process analysis shows that chemistry will be enhanced by ARF. Instead, ARF decreases ozone through physical processes.*

**Response:**

Thanks for the reviewer's suggestion. We have deleted this sentence in the revised manuscript.

5. *Line 260: "is" should be "are". Please do proof-reading throughout the text.*

**Response:**

This sentence has been deleted in the revised manuscript. According to the reviewer's comments, proof-reading has been conducted through the whole revised manuscript.

6. *Line 310: It is Okay to use model levels (e.g., 12 levels), but it will be better to add model height in meters as well.*

**Response:**

Thanks for reviewer's suggestion. We have added the model height in meters in the revised manuscript. (Page 12-13, Line 320, Line 323-325, Line 334-335)

7. *Lines 326-327: why do you need this statement?*

**Response:**

Analyzing Fig. 8c we can conclude that ARF promotes the O<sub>3</sub> chemical production with a positive mean value of 0.72 ppb h<sup>-1</sup>. The enhanced O<sub>3</sub> precursors due to ARF can promote the chemical production of O<sub>3</sub>. According to the reviewer's comment, we have deleted this statement in the revised manuscript.

8. *Lines 327-328: Please provide evidence to support this conclusion.*

**Response:**

The typical VOCs/NO<sub>x</sub> ratio is calculated to classify sensitivity regimes and to indicate the possible O<sub>3</sub> responses to changes in VOCs and/or NO<sub>x</sub> concentrations. O<sub>3</sub> production is VOC-limited if the ratio is less than 4, and it is NO<sub>x</sub>-limited if the ratio is larger than 15 (Edson et al., 2017; Li et al., 2017). The ratio of VOCs/NO<sub>x</sub> ranging around 4-15 indicates a transitional regime, where ozone is nearly equally sensitive to each species (Sillman, 1999). As shown in Fig. R1(a-f), O<sub>3</sub> are mainly formed under VOC-limited and transition regimes in CAPAs, which means that the increased concentrations of VOCs and NO<sub>x</sub> are favorable for ozone chemical production. As shown in Fig. R1(g-i) and (j-l), both the surface concentrations of VOCs and NO<sub>x</sub> are increased when the impacts of ARF are considered. Thus, the contribution of CHEM in NOAPI is larger than that in NOALL. Similar results can also be found in Gao et al. (2018).

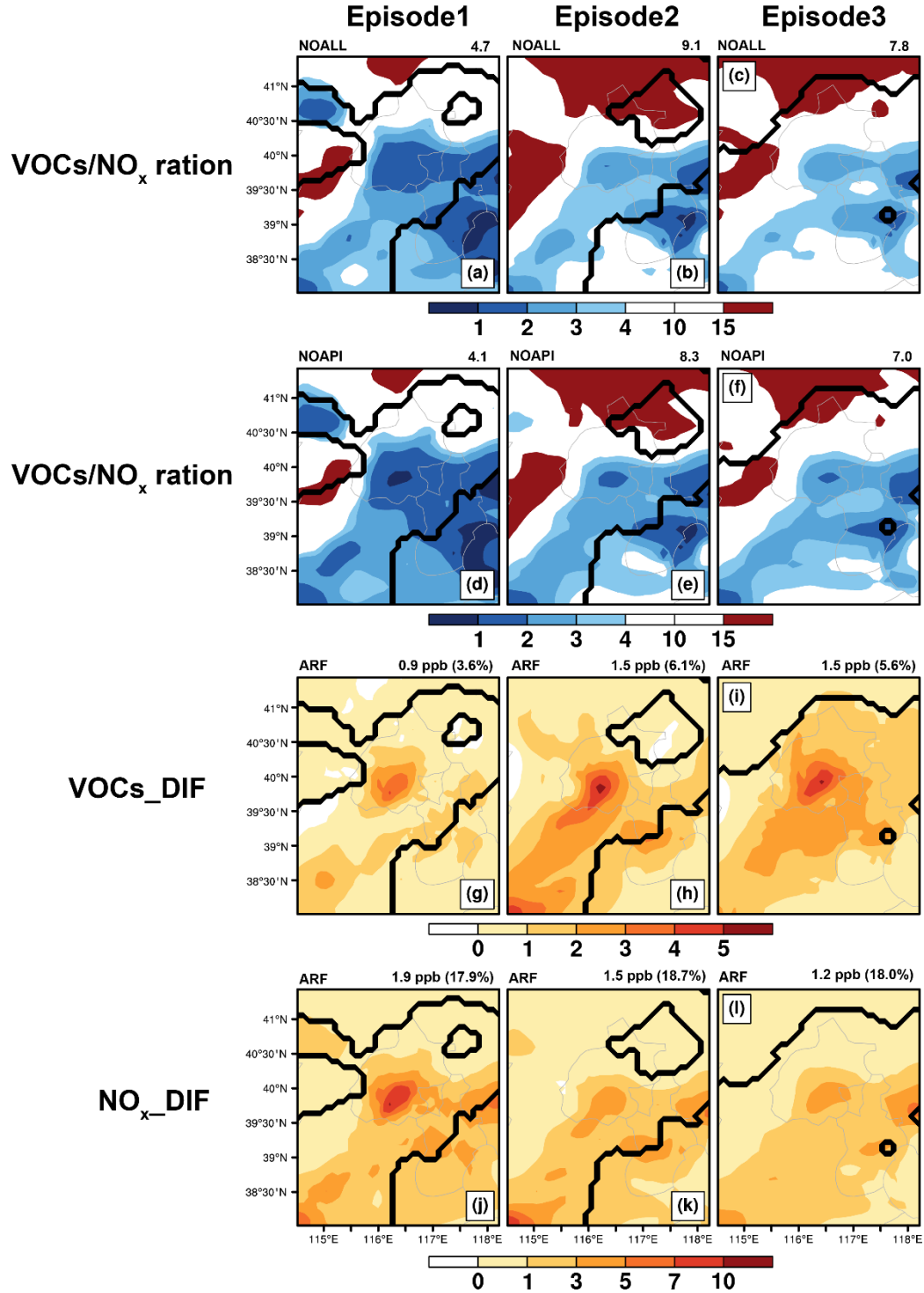


**Figure R1.** The ratios of VOCs/NO<sub>x</sub> calculated from (a-c) NOALL, and (d-f) NOAPI. The changed surface-layer concentrations of (g-i) VOCs and (j-l) NO<sub>x</sub> (NO<sub>2</sub>+NO, ppb) caused by ARF during the daytime (08:00-17:00 LST) from Episode1 to Episode3. The calculated values averaged over CAPAs are also shown at the top of each panel.

9. *Discussion. I think the authors should do some comparisons between your results with previous studies. This is important for readers to better understand your case study results. Moreover, how about the applicability of the calculated ROP of -0.14*

*ppb ( $\mu\text{g m}^{-3}$ )<sup>-1</sup>?*

**Response:**

According to the comments of Reviewer#2, we conduct another two complex air pollution episodes (8-13 July 2015 and 5-11 June 2016) in this region to draw the general conclusions. The three episodes feature a similar variation pattern, and the detailed information can be found in section 4. (**Page 9-13, Line 223-352**). Meanwhile, a discussion about the impacts of secondary organic aerosols (SOA) is also added in the section 5 (**Page 14-15, Line 391-401**).

Thanks to the reviewer's comments. As the relationship between O<sub>3</sub> and PM<sub>2.5</sub> is non-linear, and the simple index of ROP can not fully represent the impacts of aerosols on surface O<sub>3</sub>, so we delete the ROP in the revised manuscript.

*10. Fig.2: It will be better to add error bars for observed PM<sub>2.5</sub> and ozone.*

**Response:**

According to the reviewer's suggestion, error bars have been added in Fig. 2 in the revised manuscript. (**Page 27**)

*11. Fig.3: what are the cities these plots for?*

**Response:**

The averaged T<sub>2</sub>, RH<sub>2</sub>, and WS<sub>10</sub> are collected from ten meteorological observation stations, and the detail information about the sites is listed in Table S1. The photolysis rates of NO<sub>2</sub> (J[NO<sub>2</sub>]) are observed in Peking University. More details are explained in section 2.3. (**Page 6**)

*12. Fig.7: what are the layers your process analysis applied for? I don't see this key information here, as well as in the text.*

**Response:**

The surface-layer, namely, first-layer O<sub>3</sub> concentrations are analyzed in Fig. 7. Thanks for reviewer's suggestion, we have added this information in the revised manuscript. (**Page 10, Line 272**)

**Reference:**

- Edson, C. T., Ivan, H.-P. and Alberto, M.: Use of combined observational- and model-derived photochemical indicators to assess the O<sub>3</sub>-NO<sub>x</sub>-VOC System sensitivity in urban areas, *Atmosphere.*, 8, 22. <https://doi.org/10.3390/atmos8020022>, 2017.
- Gao, J. H., Zhu, B., Xiao, H., Kang, H. Q., Pan, C., Wang, D. D., and Wang, H. L.: Effects of black carbon and boundary layer interaction on surface ozone in Nanjing, China, *Atmos. Chem. Phys.*, 18, 7081–7094, <https://doi.org/10.5194/acp-18-7081-2018>, 2018.
- Li, K., Chen, L., Ying, F., White, S. J., Jang, C., Wu, X., Gao, X., Hong, S., Shen, J., Azzi, M. and Cen, K.: Meteorological and chemical impacts on ozone formation: a case study in Hangzhou, China, *Atmos. Res.*, 196, <https://doi.org/10.1016/j.atmosres.2017.06.003>, 2017.
- Sillman, S.: The relation between ozone, NO<sub>x</sub> and hydrocarbons in urban and polluted rural environments, *Atmos. Environ.*, 33, 1821-1845, [https://doi.org/10.1016/S1352-2310\(98\)00345-8](https://doi.org/10.1016/S1352-2310(98)00345-8), 1999.

**Thank you very much for your comments and suggestions.**

## Response to Comments of Reviewer #2

(comments in *italics*)

**Manuscript number:** acp-2021-119

**Title:** Impacts of aerosol-photolysis interaction and aerosol-radiation feedback on surface-layer ozone in North China during a multi-pollutant air pollution episode

*In this study, Yang et al. investigate the impact of aerosol-radiation interactions on O<sub>3</sub> formation during a multi-pollutant air pollution episode in Northern China. Additionally, the study uses process analysis to analyze how the aerosol-radiation interactions affect O<sub>3</sub> through various physical and chemical mechanisms. This is an interesting research topic with valid research methods and an overall well written and well-structured manuscript. However, the period of analysis is far too short (i.e., 7 days) to robustly quantify the impact of aerosol-radiation impacts in this region or to describe any variability. Additionally, the time period analyzed appears somewhat arbitrary and is nearly a decade removed from current conditions. For these reasons, the manuscript is not currently at the scientific level of the Atmospheric Chemistry and Physics Journal. However, this manuscript would be suitable for publication in ACP if either it is restructured to focus on how the methods used are unique and different from past work or if the authors investigate longer periods to generate more robust analysis and conclusions. Please find my major and minor comments below.*

### **Response:**

Thanks to the reviewer for the valuable comments and suggestions which are very helpful for us to improve our manuscript. We have revised the manuscript carefully, as described in our point-to-point responses to the comments.

The major innovation of this study is that it is the first time to quantify the respective/combined contributions of aerosol-photolysis interaction (API) and aerosol-radiation feedback (ARF) on O<sub>3</sub> concentrations during multi-pollutant air pollution episodes characterized by high O<sub>3</sub> and PM<sub>2.5</sub> levels. According to the reviewer's comments, another two complex air pollution episodes are also analyzed for generating general conclusions, and we find that API is the dominant factor for O<sub>3</sub> reduction related to aerosol-radiation interactions during all the simulated episodes (Episode1: 28 July-3 August 2014; Episode2: 8-13 July 2015; Episode3: 5-11 June 2016).

### **Major Comments:**

1. *The novelty of this study is that it is the first time that API and ARF are investigated for synchronous occurrences of high PM<sub>2.5</sub> and O<sub>3</sub> concentrations. This is a rather broad research question to be focused on only one region and one very minor time period. Why do the authors not conduct simulations for either several of these small pollution episodes in this region or for similar episodes in other locations in China?*

### **Response:**

The high-resolution WRF-Chem model has been widely applied to investigate the evolution mechanisms of air pollutants during short time periods (Gao et al., 2016; Qiu et al., 2017; Gao et

al., 2018; Wang et al., 2020). Gao et al. (2016) summarized the general conclusion that haze events were mainly caused by high emissions of air pollutants and unfavorable weather conditions in North China Plain (NCP) by analyzing a simulated pollution episode from WRF-Chem during 14-24 January 2010. According to the results from WRF-Chem, Qiu et al. (2017) reported that the direct radiative effects of scattering aerosols were greater than that of absorbing aerosols in NCP during 21-27 February 2014. Gao et al. (2018) found that the interactions between black carbon and planetary boundary layer (PBL) could influence the surface O<sub>3</sub> concentration in Nanjing during 17 October 2015 by using the process analysis in WRF-Chem.

According to the reviewer's comments, another two complex air pollution episodes (8-13 July 2015 and 5-11 June 2016) in this region are also selected to conduct simulations for generating general conclusions.

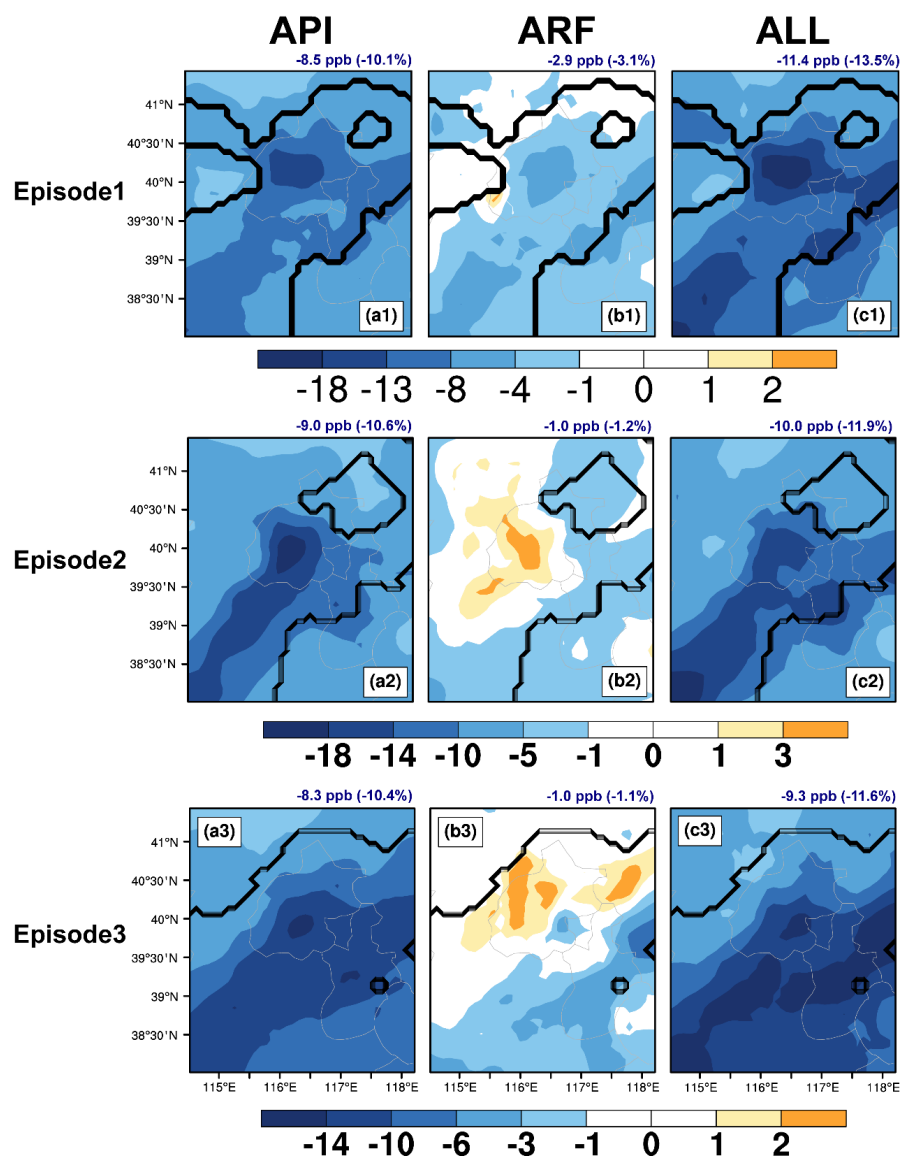


**Figure R1.** The changes in surface-layer ozone due to (a) aerosol-photolysis interaction (API), (b) aerosol-radiation feedback (ARF), and (c) the combined effects (ALL, defined as API+ARF) in the daytime (08:00-17:00 LST) during 28 July to 3 August 2014 (Episode1), 8-13 July 2015 (Episode2) and 5-11 June 2016 (Episode3). The region sandwiched between two black lines is defined as the complex air pollution areas (CAPAs) where the mean daily



PM<sub>2.5</sub> and MDA8 O<sub>3</sub> concentrations in BASE case are larger than 75  $\mu\text{g m}^{-3}$  and 80 ppb. The calculated mean changes (percentage changes) averaged over CAPAs are also shown at the top of each panel.

Simulated air pollutants (PM<sub>2.5</sub> and O<sub>3</sub>) and meteorological variables (T<sub>2</sub>, RH<sub>2</sub>, WS<sub>10</sub>, and J[NO<sub>2</sub>]) during 28 July to 3 August 2014 (Episode1), 8-13 July 2015 (Episode2) and 5-11 June 2016 (Episode3) are compared with observations. In general, both the observed meteorological parameters and pollutant concentrations can be reasonably reproduced by the model, with correlation coefficients (R) of 0.56~0.98 and normalized mean bias (NMB) of -12.0%~+33.4%. More details about the model evaluation are listed in the section 3 in the revised manuscript (**Page 7-8, Line 181-212**). The impacts of aerosol radiation effects on meteorological variables can be found in section 4.1 and 4.2 in the revised manuscript during these three episodes (**Page 9-10, Line 223-254**).

As shown in Fig. R1(a1-a3), API alone leads to overall surface O<sub>3</sub> decreases over the entire domain with average reductions of 8.5 ppb (10.1%), 9.0 ppb (10.6%) and 8.3 ppb (10.4%) over CAPAs in the three episodes, respectively. The changes can be explained by the substantially diminished UV radiation due to aerosol loading, which significantly weakens the efficiency of photochemical reactions and restrains O<sub>3</sub> formation. However, the decreased surface O<sub>3</sub> concentrations due to ARF are only 2.9 ppb (3.1%, Fig. R1(b1)), 1.0 ppb (1.2%, Fig. R1(b2)) and 1.0 ppb (1.1%, Fig. R1(b3)) for the three episodes, which indicates that API is the dominant way for O<sub>3</sub> reduction related to aerosol-radiation interactions. Fig. R1(c1-c3) presents the combined effects of API and ARF. Generally, aerosol-radiation interactions decrease the surface O<sub>3</sub> concentrations by 11.4 ppb (13.5%), 10.0 ppb (11.9%) and 9.3 ppb (11.6%) averaged over CAPAs in the three episodes, respectively. (**Page 10, Line 256-269**)

2. *Given that government controls have substantially changed emissions in the last decade and will continue into future, how will this research remain relevant in the future or how relevant is it to today's air pollution in China, since the period examined is 7 years ago?*

**Response:**

The stringent Air Pollution Action Plan has been released by the Chinese government in September 2013 to improve the PM<sub>2.5</sub> air quality. Although the concentrations of PM<sub>2.5</sub> are decreasing, the concentrations of PM<sub>2.5</sub> still exceed 35  $\mu\text{g m}^{-3}$ , and the O<sub>3</sub> levels have continued to increase (Dai et al., 2021). Many studies have found that the decreased PM<sub>2.5</sub> can be one of the important causes leading to the increase in O<sub>3</sub> (Li et al. 2019; Shao et al., 2021). Li et al. (2019) pointed out that the concentrations of PM<sub>2.5</sub> were decreased by 40% in North China Plain from 2013 to 2017, which reduced the sink of HO<sub>2</sub> on aerosol surfaces and resulted in the increase in O<sub>3</sub> by analyzing simulation results from the GEOS-Chem model. Meanwhile, the concentrations of O<sub>3</sub> can also be influenced by aerosol-radiation interactions, including aerosol-photolysis interaction and aerosol-radiation feedback, which have not been systematically analyzed. The quantification of the impacts of aerosols on O<sub>3</sub> is important to well understand the co-benefits associated with reductions in both aerosols and O<sub>3</sub>.

In this study, we investigate the impacts of aerosol-radiation interactions on surface O<sub>3</sub>, and find that the combined impacts of weakened photolysis rates and changed meteorological conditions reduce surface-layer O<sub>3</sub> concentrations by up to 9.3~11.4 ppb. The result can imply that the

decreases in PM<sub>2.5</sub> can lead to the increase in O<sub>3</sub> due to the weakened aerosol-radiation interactions, which indicates that if the government controls the anthropogenic emissions in future by using the same strategy, higher O<sub>3</sub> will be observed. The result can further emphasize the importance of tighter controls in O<sub>3</sub> precursors (e.g., VOCs) to counteract the increased O<sub>3</sub> caused by weakened aerosol-radiation interactions. Therefore, the contributions of different mitigation strategies with the impacts of aerosol-radiation interactions to O<sub>3</sub> air quality will be discussed detailedly in our future work.

3. *Is the focus of this research the method in which API and ARF are investigated or the impact of API and ARF in North China? If it is the former than the authors need to reword the abstract, conclusions, and objectives to make it clear that this study is a “proof-of-concept” study on how to best investigate API and ARF in high O<sub>3</sub> and PM<sub>2.5</sub> episodes. If the focus is the latter, the authors need to do additional simulations of other high multi-pollutant episodes, perhaps some closer to current conditions and others in the mid 2000s to see if there is change over time or to make the analysis and conclusions more robust.*

**Response:**

This study mainly focuses on the impacts of API and ARF in North China. According to the reviewer’s comments, another two complex air pollution episodes (8-13 July 2015 and 5-11 June 2016) in this region are also selected to conduct simulations for generating general conclusions. The impacts of API and ARF on O<sub>3</sub> are shown in Fig. R1, and API is the dominant factor for O<sub>3</sub> reduction related to aerosol-radiation interactions in these three episodes.

4. *Does this version of WRF-Chem’s CBM-Z and MOSAIC modules have a volatility basis set (VBS) option to simulate secondary organic aerosols and if so is it used? Given that, this is a high O<sub>3</sub> and PM<sub>2.5</sub> episode there should be a substantial amount of secondary organic aerosol from abundant oxidants and precursors that may be missed in the model without an advanced SOA scheme. How do the author’s address the impact of SOA on their conclusions?*

**Response:**

The selected gas-phase chemical mechanism (CBM-Z) and the aerosol model (MOSAIC) in this study do not consider the impacts of secondary organic aerosols (SOA). The same schemes have been widely used in many other studies, which mainly focus on the impacts of aerosol-radiation interactions on air pollutants in North China (Ding et al., 2016; Gao et al., 2016; Qiu et al., 2017; Chen et al., 2019; Zhou et al., 2019; Gao et al., 2020).

Thanks for the reviewer’s suggestion, and we will consider the impacts of SOA in our future works. A discussion about the impacts of SOA has been added in the revised manuscript as follows: “Gao et al. (2017) added some SOA formation mechanisms into the MOSAIC module by using the volatility basis set (VBS) in WRF-Chem and found that the surface PM<sub>2.5</sub> concentrations in urban Beijing were reduced by 1.9 µg m<sup>-3</sup> due to the weakened ARF effect during Asia-Pacific Economic Cooperation (APEC). Similar magnitude can also be found in Zhou et al. (2019) (-1.8 µg m<sup>-3</sup>) who did not consider the impacts of SOA in WRF-Chem when analyzing the impacts of weakened ARF on PM<sub>2.5</sub> during APEC. Therefore, more work should be conducted to explore the impacts of ARF on PM<sub>2.5</sub> and O<sub>3</sub> concentrations under consideration of SOA in future.” (Page 14-15, Line 391-401)

5. *The authors are investigating aerosol radiation interactions, but the authors do not evaluate the model's performance against either radiation balance datasets or aerosol optical depth. Since these parameters are more important than surface evaluations of air pollutants to understanding API and ARF, the authors should evaluate their model configuration against satellite AOD and radiation variables such as MODIS or CERES-EBAF.*

**Response:**

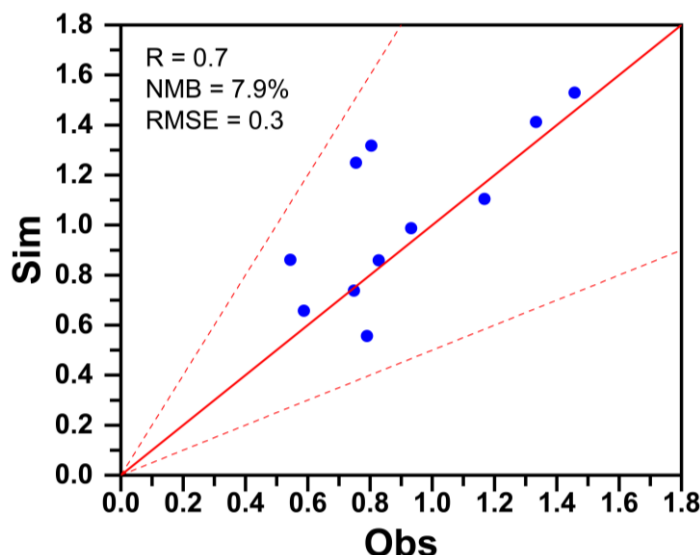


**Figure R2.** Comparison of observed and simulated AOD at 550 nm in Beijing (39.98°N, 116.38°E). The observed AOD during the three episodes are collected from AERONET.

Previous studies found that MODIS retrievals tended to overestimate AOD in the NCP during polluted events compared with AERONET AOD (Gao et al., 2015; Li et al., 2016). Therefore, we mainly focus on the comparisons between simulated AOD values and AERONET observations in this work. Figure R2 shows the correlation between observed and simulated AOD at 550 nm in Beijing. In the WRF-Chem model, the AOD at 550 nm are calculated by using the values at 400 and 600 nm according to the Angstrom exponent. Analyzing Fig. R2, the model can reproduce the observed AOD with  $R$  of 0.7 and NMB of 7.9%.

According to the reviewer's suggestion, the description of the model evaluation between observed and simulated AOD is added in the revised manuscript (**Page 8, Line 190-193**), and Figure R2 is also added in the supporting information (**Figure S1**).

6. *Are there only three meteorological observation stations in the domain against? If so, why do the authors not also validate their meteorological performance against gridded products like the Climate Research Unit (CRU) datasets to ensure their performance statistics are robust?*

**Response:**

Thanks to the reviewer's comments. More meteorological observations in the analyzed domain (Table R1) have been used to validate the model results, and the locations of each site are shown in Fig. R3.

Figure R4 shows the time series of observed and simulated  $T_2$ ,  $RH_2$ ,  $WS_{10}$  and  $J[NO_2]$  during

the three episodes. The observed  $T_2$ ,  $RH_2$ ,  $WS_{10}$  are averaged over the ten meteorological observation stations, and the  $J[NO_2]$  are measured at Peking University. Most of the monitored  $J[NO_2]$  in Episode3 are unavailable, so the comparison of  $J[NO_2]$  in Episode3 is not shown. Generally, the model can depict the temporal variations of  $T_2$  fairly well with  $R$  of 0.98 and the mean bias (MB) of  $-1.9 \sim -0.9$  °C. For  $RH_2$ , the  $R$  and MB are 0.91~0.97 and  $-4.0\% \sim 1.9\%$ , respectively. Although WRF-Chem model overestimates  $WS_{10}$  with the MB of  $0.6 \sim 0.9$  m s<sup>-1</sup>, the  $R$  for  $WS_{10}$  is 0.70~0.89 and the root-mean-square error (RMSE) is  $0.9 \sim 1.5$  m s<sup>-1</sup>, which is smaller than the threshold of model performance criteria (2 m s<sup>-1</sup>) proposed by Emery et al. (2001). The positive bias in wind speed can also be reproduced in other studies (Zhang et al., 2010; Gao et al., 2015; Liao et al., 2015; Qiu et al., 2017). The predicted  $J[NO_2]$  agrees well with the observations with  $R$  of 0.97~0.98 and NMB of 6.8%~6.9%.

According to the reviewer's comments, we have modified the model evaluation in the revised manuscript. (Page 8, Line 195-208)

The gridded products like the Climate Research Unit (CRU) datasets covers a large area and a longtime period, which aims to improve scientific understanding of the climate system and its interactions with society. However, the spatial ( $0.5^\circ \times 0.5^\circ$ ) and temporal (monthly) resolution may be too coarse to validate the model performance for generating robust results.

**Table R1.** Locations of the ten stations from NOAA's National Climatic Data Center used in this study.

Station	Latitude (°)	Longitude (°)
Yuxian	39.833	114.567
Fengning	41.2	116.633
Zhangjiakou	40.783	114.883
Huailai	40.417	115.5
Chengde	40.967	117.917
Beijing	40.08	116.585
Tianjin	39.1	117.167
Binhai	39.124	117.346
Tangshan	39.65	118.1
Baoding	38.733	115.483

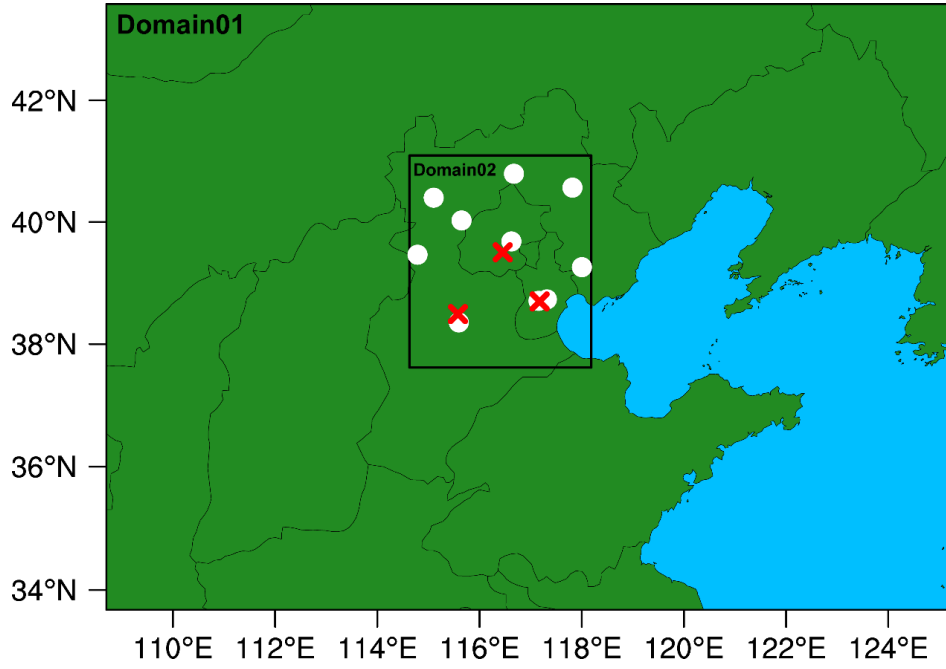


**Figure R3.** Map of the two WRF-Chem modeling domains with the locations of meteorological (white dots) and environmental (red crosses) observation sites used for model evaluation.

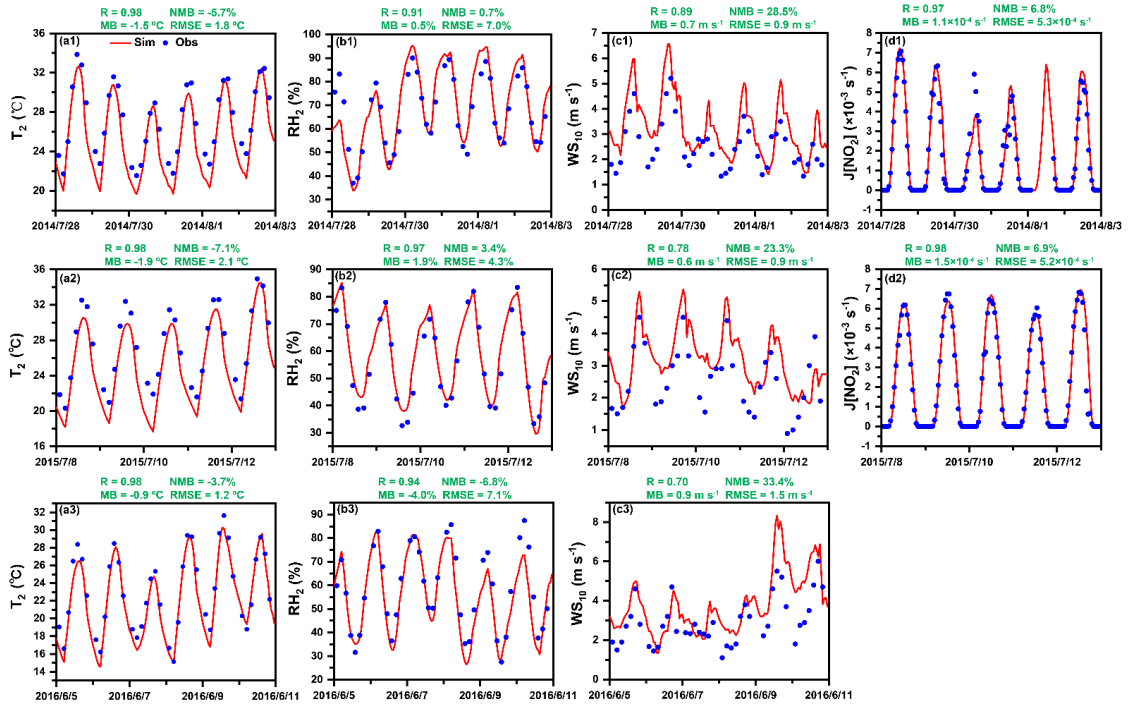


**Figure R4.** Time series of 3-hourly observed (blue dots) and hourly simulated (red lines) (a) 2-m temperature ( $T_2$ ), (b) 2-m relative humidity ( $RH_2$ ), (c) wind speed at 10 m ( $WS_{10}$ ) averaged over ten meteorological observation stations, and (d) surface photolysis rate of  $NO_2$  ( $J[NO_2]$ ) during 28 July to 3 August 2014 (Episode1, a1-d1), 8-13 July 2015 (Episode2, a2-d2) and 5-11 June 2016 (Episode3, a3-c3). The calculated correlation coefficient (R), mean bias (MB), normalized mean bias (NMB) and root-mean-square error (RMSE) are also shown.

7. Given that interactions between  $O_3$  and  $PM_{2.5}$  are non-linear, how do the authors justify using a simple ratio value (i.e., ROP) to relate these interactions? If this ratio

*does not account for non-linearity, how useful is this value?*

**Response:**

Thanks to the reviewer's suggestion. As the relationship between  $O_3$  and  $PM_{2.5}$  is non-linear, and the simple index of ROP can not fully represent the impacts of aerosols on surface  $O_3$ , so we delete the ROP in the revised manuscript.

8. *The axis labels and legends of Figure 7 are difficult to read. Either each panel should be larger overall or the font sizes of the axes and legends need increased.*

**Response:**

According to the reviewer's suggestion, we have modified the axis labels and legends of Figure 7 and the other figures in the revised manuscript. (Page 32)

**Minor Comments:**

- 1) *In the abstract, there is no context for the values listed. Further reading into the manuscript reveals that these values are the averages in the areas of the complex air pollution areas. The authors should briefly state that these values are for daytime average changes in complex air pollution areas in the abstract. I would also suggest adding a more processed based explanation of the changes in atmospheric state rather than simply listing a long series of values. For example, the authors could state something similar to the following: "Aerosol radiation interactions lead to shortwave dimming at the earth's surface of X, which reduce photolysis rates by X. The dimming stabilizes the atmosphere via surface cooling of X, which reduces PBL height by X. The stabilized atmosphere increases saturation in the lower atmosphere by X. etc...."*

**Response:**

According to the reviewer's suggestion, we have revised the explanation in the abstract as follows: "Our results show that aerosol-radiation interactions decreased the daytime shortwave radiation at surface by 92.4~100.3 W m<sup>-2</sup> averaged over the complex air pollution areas in these three episodes. The dimming effect reduced the near-surface photolysis rates of J[NO<sub>2</sub>] and J[O<sup>1</sup>D] by  $1.8 \times 10^{-3}$ ~ $2.0 \times 10^{-3}$  s<sup>-1</sup> and  $5.7 \times 10^{-6}$ ~ $6.3 \times 10^{-6}$  s<sup>-1</sup>, respectively. However, the daytime shortwave radiation in the atmosphere was increased by 72.8~85.2 W m<sup>-2</sup>, which made the atmosphere more stable. The stabilized atmosphere decreased the planetary boundary layer height and 10 m wind speed by 129.0~249.0 m and 0.05~0.12 m s<sup>-1</sup>, respectively." (Page 2, Line 25-33)

- 2) *Make it clear throughout the manuscript when you are referring to surface level  $O_3$  and  $PM_{2.5}$ .*

**Response:**

According to the reviewer's suggestion, we have revised the expressions in the whole manuscript.

- 3) *Lines 179-181: The missing  $PM_{2.5}$  could also be from missing SOA formation pathways, as mentioned above, if no advanced SOA formulations are used.*

**Response:**

Thanks for your suggestion. The selected aerosol model (MOSAIC) in this study does not

consider the impacts of secondary organic aerosols (SOA). We have deleted this sentence in the revised manuscript.

- 4) *Is “downward shortwave radiation in the atmosphere” the SWDNT variable from WRF-Chem? If so, the name of this variable is “downward shortwave radiation at the top of the atmosphere”.*

**Response:**

Thanks for your comments. In the WRF-Chem model, SWDNT (SWUPT) means the download (upward) shortwave radiation at the top of atmosphere, and SWDNB (SWUPB) represents the download (upward) shortwave radiation at the surface. According to Zhao et al. (2011), the shortwave radiation in the atmosphere (ATM\_SW) can be calculated as the difference between TOP\_SW (the net shortwave radiation at the top of atmosphere, i.e., SWDNT minus SWUPT) and BOT\_SW (the net shortwave radiation at the surface, i.e., SWDNB minus SWUPB).

According to the reviewer’s suggestion, we have changed the expressions of BOT\_SW (shortwave radiation at the surface) and ATM\_SW (shortwave radiation in the atmosphere) in the whole revised manuscript.

- 5) *Lines 217-218: If ATM\_SW is the SWDNT variable, what is causing it to increase? SWDNT is usually controlled by the solar constant. Is it possible this is reflected upward shortwave (SWUPT)?*

**Response:**

ATM\_SW represents the shortwave radiation in the atmosphere, and it can be calculated by the following equation:  $ATM\_SW = (SWDNT - SWUPT) - (SWDNB - SWUPB)$ .

- 6) *Lines 248-249: This should be revised to make it clearer that ARF primarily impacts O<sub>3</sub> through changing the NO<sub>x</sub> distribution.*

**Response:**

According to the comments of Reviewer#1, we have deleted this sentence.

- 7) *Lines 270-281: Is VMIX increasing surface O<sub>3</sub> because it is mixing down higher O<sub>3</sub> concentrations from aloft or because vertical mixing is suppressed due to a stable atmosphere?*

**Response:**

VMIX increases the surface O<sub>3</sub> concentrations by transporting the higher O<sub>3</sub> from aloft to the surface layer. Similar results can also be found in previous studies (Tang et al., 2017; Xing et al., 2017; Gao et al., 2018).

- 8) *Lines 282-294: Why does the VMIX contribution increase because of API?*

**Response:**

Analyzing the vertical profiles of the differences in contributions from each physical/chemical process to hourly O<sub>3</sub> variations caused by API in Fig. 8(b), we found that the contribution of VMIX\_DIF is negative in the aloft (among the 9<sup>th</sup> and the 13<sup>th</sup> layers), while it turns to be positive at the lower seven layers, and the positive contribution increases as the height decreases. The positive variation in VMIX due to API may be associated with the different vertical gradient of O<sub>3</sub>

between BASE and NOAPI cases.

Similar results can also be found in Gao et al. (2020), who concluded that the increased vertical gradients of O<sub>3</sub> due to API could enhance the vertical entrainment.

9) *Lines 295-301: Explain why VMIX\_DIF and CHEM\_DIF are positive during the day due to ARF.*

**Response:**

When the impacts of ARF are considered, PBLH is decreased over CAPAs (Fig. S4(a3-c3)), which indicates that the suppressed PBL in NOAPI restrains the vertical turbulence and prevents O<sub>3</sub> being transported from aloft to surface, resulting in lower O<sub>3</sub> concentrations at surface when comparing with the simulation results of NOALL. However, as the evolution in boundary layer during the daytime, more O<sub>3</sub> can be diffused from the upper layers to the surface in NOAPI, and the differences in hourly variation in surface O<sub>3</sub> due to vertical mixing between NOAPI and NOALL are positive. Similar results can also be found in Gao et al. (2018).

The typical VOCs/NO<sub>x</sub> ratio is calculated to classify sensitivity regimes and to indicate the possible O<sub>3</sub> responses to changes in VOCs and/or NO<sub>x</sub> concentrations. O<sub>3</sub> production is VOC-limited if the ratio is less than 4, and it is NO<sub>x</sub>-limited if the ratio is larger than 15 (Edson et al., 2017; Li et al., 2017). The ratio of VOCs/NO<sub>x</sub> ranging around 4-15 indicates a transitional regime, where ozone is nearly equally sensitive to each species (Sillman, 1999). As shown in Fig R5(a-f), O<sub>3</sub> are mainly formed under the VOC-limited and the transition regimes in CAPAs, which means that the increased concentrations of VOCs and NO<sub>x</sub> are favorable for ozone chemical production. As shown in Fig. R5(g-i) and (j-l), both the surface concentrations of VOCs and NO<sub>x</sub> are increased when the impacts of ARF are considered. Thus, the contribution of CHEM in NOAPI is larger than that in NOALL. Similar results can also be found in Gao et al. (2018).



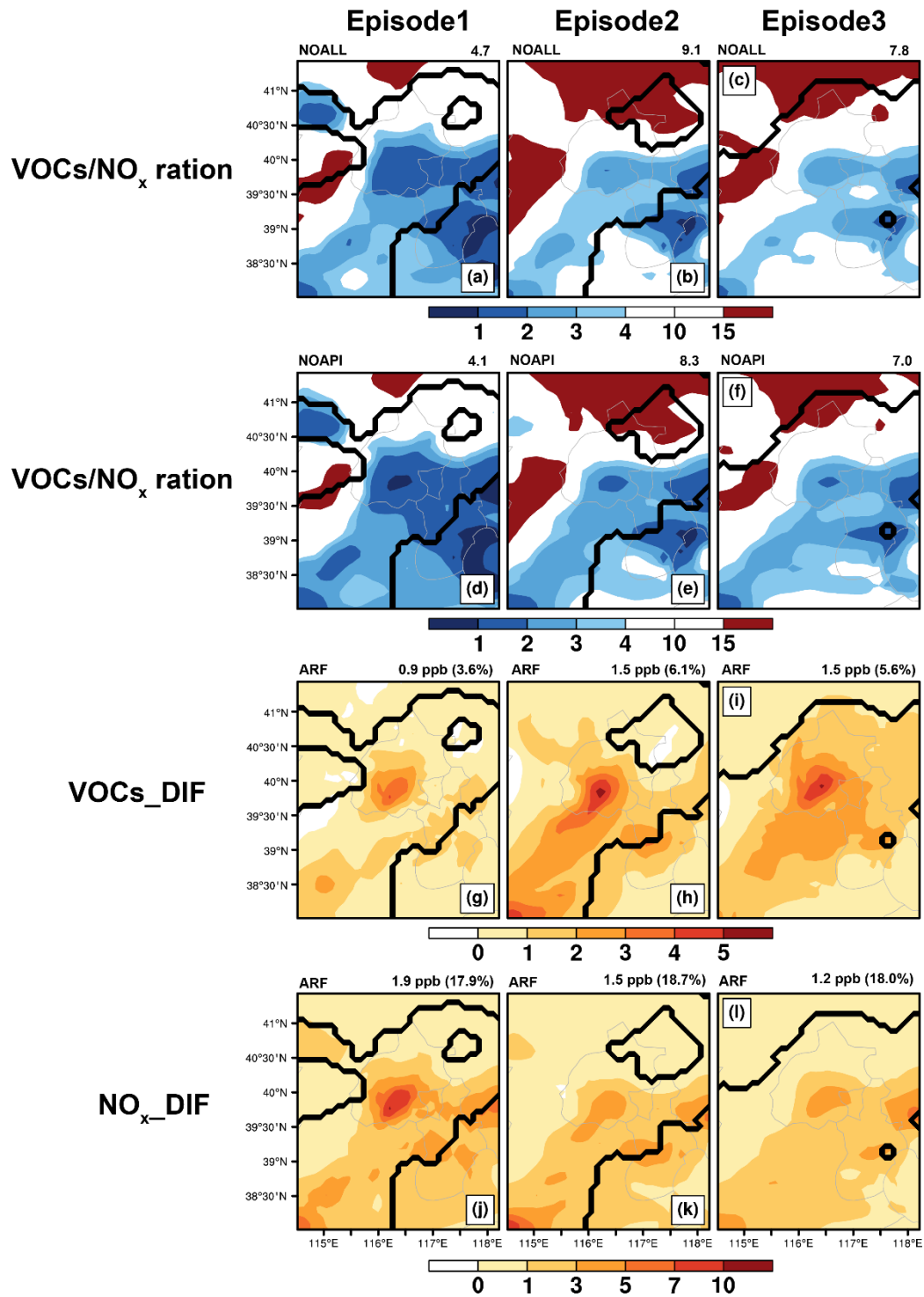


**Figure R5.** The ratios of VOCs/NO<sub>x</sub> calculated from (a-c) NOALL, and (d-f) NOAPI. The changed surface-layer concentrations of (g-i) VOCs and (j-l) NO<sub>x</sub> (NO<sub>2</sub>+NO, ppb) caused by ARF during the daytime (08:00-17:00 LST) from Episode1 to Episode3. The calculated values averaged over CAPAs are also shown at the top of each panel.

10) Lines 315-316: Explain how different vertical O<sub>3</sub> gradients can cause this change.

**Response:**

Since the VMIX is closely dependent on atmospheric turbulence and vertical gradients of O<sub>3</sub> concentration. The API will increase vertical gradients of O<sub>3</sub> to enhance the vertical entrainment

(Gao et al., 2020).

**Line Comments:**

1) *Line 49: This should be “Earth’s radiative balance” or “Earth’s energy balance”*

**Response:**

Thanks for your suggestion. We have changed the expression in the revised manuscript. (Page 3, Line 49)

2) *Lines 54-56: Are these studies all focused on China? If so, state that in the sentence. Change “were” to “are”.*

**Response:**

According to the reviewer’s suggestion, we have changed the expression in the revised manuscript. (Page 3, Line 55)

3) *Lines 56-63: State the domain and time period of Gao et al., (2015) at the beginning of this statement rather than the end*

**Response:**

According to the reviewer’s suggestion, we have changed the expression in the revised manuscript. (Page 3, Line 56-63)

4) *Line 66: Add “the” before North China Plain*

**Response:**

Thanks for your suggestion. We have added the “the” before North China Plain in the revised manuscript. (Page 3, Line 66)

5) *Lines 66-67: If this is referring to surface PM<sub>2.5</sub> concentrations, add “surface” before PM<sub>2.5</sub> concentrations.*

**Response:**

Thanks for your suggestion. We have added the “surface” before PM<sub>2.5</sub> concentrations in the revised manuscript. (Page 3, Line 66)

6) *Line 204: should be “attention”*

**Response:**

Thanks for your suggestion. We have changed the expression in the revised manuscript. (Page 9, Line 216)

7) *Line 256: Center align the equation.*

**Response:**

This equation has been deleted.

8) *Line: 259: Why are there parentheses in the units?*

**Response:**

This sentence has been deleted.

9) *Lines 288-289: This sentence is a little confusing. Is Net\_DIF the sum of CHEM\_DIF, VMIX\_DIF, and ADV\_DIF? If so, state that explicitly and then indicate what Net\_DIF describes.*

**Response:**

Thanks for your suggestion. We have defined the NET\_DIF in the revised manuscript. (Page 11, Line 297)

10) *Line 321: Remove “in the”*

**Response:**

According to the reviewer’s suggestion, we have deleted it in the revised manuscript.

11) *Line 361: Remove “the contribution from VMIX and”*

**Response:**

According to the reviewer’s suggestion, we have deleted it in the revised manuscript.

12) *Line 373: Either “A recent study” or “Recent studies have”*

**Response:**

According to the reviewer’s suggestion, we have changed the expression in the revised manuscript. (Page 14, Line 385)

**Reference:**

Dai, H., Zhu, J., Liao, H., Li, J., Liang, M., Yang, Y., and Yue, X.: Co-occurrence of ozone and PM<sub>2.5</sub> pollution in the Yangtze River Delta over 2013–2019: Spatiotemporal distribution and meteorological conditions, *Atmos. Res.*, 249, 105363, 2021.

Ding, A. J., Huang, X., Nie, W., Sun, J. N., Kerminen, V. M., Petäjä, T., Su, H., Cheng, Y. F., Yang, X. Q., Wang, M. H., Chi, X. G., Wang, J. P., Virkkula, A., Guo, W. D., Yuan, J., Wang, S. Y., Zhang, R. J., Wu, Y. F., Song, Y., Zhu, T., Zilitinkevich, S., Kulmala, M., and Fu, C. B.: Enhanced haze pollution by black carbon in megacities in China, *Geophys. Res. Lett.*, 43, 2873–2879, <https://doi.org/10.1002/2016gl067745>, 2016.

Edson, C. T., Ivan, H.-P. and Alberto, M.: Use of combined observational- and model-derived photochemical indicators to assess the O<sub>3</sub>-NO<sub>x</sub>-VOC System sensitivity in urban areas, *Atmosphere.*, 8, 22. <https://doi.org/10.3390/atmos8020022>, 2017.

Emery, C., Tai, E., and Yarwood, G.: Enhanced meteorological modeling and performance evaluation for two Texas ozone episodes, in: Prepared for the Texas Natural Resource Conservation Commission, ENVIRON International Corporation, Novato, CA, USA, 2001.

Gao, J. H., Zhu, B., Xiao, H., Kang, H. Q., Pan, C., Wang, D. D., and Wang, H. L.: Effects of black carbon and boundary layer interaction on surface ozone in Nanjing, China, *Atmos. Chem. Phys.*, 18, 7081–7094, <https://doi.org/10.5194/acp-18-7081-2018>, 2018.

Gao, J., Li, Y., Zhu, B., Hu, B., Wang, L., and Bao, F.: What have we missed when studying the impact of aerosols on surface ozone via changing photolysis rates?, *Atmos. Chem. Phys.*, 20, 10831–10844,

- <https://doi.org/10.5194/acp-20-10831-2020>, 2020.
- Gao, M., Carmichael, G. R., Wang, Y., Saide, P. E., Yu, M., Xin, J., Liu, Z., and Wang, Z.: Modeling study of the 2010 regional haze event in the North China Plain, *Atmos. Chem. Phys.*, 16, 1673–1691, doi:10.5194/acp-16-1673-2016, 2016.
- Gao, M., Liu, Z., Wang, Y., Lu, X., Ji, D. and Wang, L.: Distinguishing the roles of meteorology, emission control measures, regional transport, and co-benefits of reduced aerosol feedbacks in “APEC” Blue, *Atmos. Environ.*, 167, 476–486, 420 doi:10.1016/j.atmosenv.2017.08.054, 2017.
- Gao, Y., Zhang, M., Liu, Z., Wang, L., Wang, P., Xia, X., Tao, M., and Zhu, L.: Modeling the feedback between aerosol and meteorological variables in the atmospheric boundary layer during a severe fog–haze event over the North China Plain, *Atmos. Chem. Phys.*, 15, 4279–4295, doi:10.5194/acp-15-4279-2015, 2015.
- Li, K., Liao, H., Zhu, J., and Moch, J. M.: Implications of RCP emissions on future PM<sub>2.5</sub> air quality and direct radiative forcing over China, *J. Geophys. Res. Atmos.*, 121, 12,985–13,008, doi:10.1002/2016JD025623, 2016.
- Li, K., Chen, L., Ying, F., White, S. J., Jang, C., Wu, X., Gao, X., Hong, S., Shen, J., Azzi, M. and Cen, K.: Meteorological and chemical impacts on ozone formation: a case study in Hangzhou, China, *Atmos. Res.*, 196, <https://doi.org/10.1016/j.atmosres.2017.06.003>, 2017.
- Li, K., Jacob, D. J., Liao, H., Shen, L., Zhang, Q., and Bates, K. H.: Anthropogenic drivers of 2013–2017 trends in summer surface ozone in China, *P. Natl. Acad. Sci. USA*, 116, 422–427, <https://doi.org/10.1073/pnas.1812168116>, 2019.
- Qiu, Y., Liao, H., Zhang, R., and Hu, J.: Simulated impacts of direct radiative effects of scattering and absorbing aerosols on surface layer aerosol concentrations in China during a heavily polluted event in February 2014, *J. Geophys. Res. Atmos.*, 122, 5955–5975, doi:10.1002/2016JD026309, 2017.
- Shao, M., Wang, W. J., Yuan, B., Parrish, D. D., Li, X., Lu, K. D., Wu, L. L., Wang, X. M., Mo, Z. W., Yang, S. X., Peng, Y. W., Kuang, Y., Chen, W. H., Hu, M., Zeng, L. M., Su, H., Cheng, Y. F., Zheng, J. Y., Zhang, Y. H.: Quantifying the role of PM<sub>2.5</sub> dropping in variations of ground-level ozone: Inter-comparison between Beijing and Los Angeles, *Sci. Total Environ.*, <https://doi.org/10.1016/j.scitotenv.2021.147712>, 2021.
- Sillman, S.: The relation between ozone, NO<sub>x</sub> and hydrocarbons in urban and polluted rural environments, *Atmos. Environ.*, 33, 1821–1845, [https://doi.org/10.1016/S1352-2310\(98\)00345-8](https://doi.org/10.1016/S1352-2310(98)00345-8), 1999.
- Tang, G. Q., Zhu, X.W., Xin, J. Y., Hu, B., Song, T., Sun, Y., Zhang, J. Q., Wang, L. L., Cheng, M. T., Chao, N., Kong, L. B., Li, X., and Wang, Y. S.: Modelling study of boundary-layer ozone over northern China – Part I: Ozone budget in summer, *Atmos. Res.*, 187, 128–137, 2017.
- Wang, T., Huang, X., Wang, Z., Liu, Y., Zhou, D., Ding, K., Wang, H., Qi, X. and Ding, A.: Secondary Aerosol Formation and its Linkage with Synoptic Conditions during Winter Haze Pollution over Eastern China, *Sci. Total Environ.*, 730, 138888, 2020.
- Xing, J., Wang, J. D., Mathur, R., Wang, S. X., Sarwar, G., Pleim, J., Hogrefe, C., Zhang, Y. Q., Jiang, J. K., Wong, D. and Hao, J. M.: Impacts of aerosol direct effects on tropospheric ozone through changes in atmospheric dynamics and photolysis rates, *Atmos. Chem. Phys.*, 17, 9869–9883, <https://doi.org/10.5194/acp-17-9869-2017>, 2017.
- Zhao, C., Liu, X., Ruby Leung, L., and Hagos, S.: Radiative impact of mineral dust on monsoon precipitation variability over West Africa, *Atmos. Chem. Phys.*, 11, 1879–1893, <https://doi.org/10.5194/acp-11-1879-2011>, 2011.
- Zhou, M., Zhang, L., Chen, D., Gu, Y., Fu, T.-M., Gao, M., Zhao, Y., Lu, X. and Zhao, B.: The impact of aerosol-radiation interactions on the effectiveness of emission control measures, *Environmental Research Letters*, 14(2), 024002, <https://doi.org/10.1088/1748-9326/aaf27d>, 2019.

**Thank you very much for your comments and suggestions.**

**Impacts of aerosol-photolysis interaction and aerosol-radiation  
feedback on surface-layer ozone in North China during a multi-  
pollutant air pollution episode<sub>s</sub>**

Hao Yang<sup>1</sup>, Lei Chen<sup>1</sup>, Hong Liao<sup>1</sup>, Jia Zhu<sup>1</sup>, Wenjie Wang<sup>2</sup>, Xin Li<sup>2</sup>

<sup>1</sup>Jiangsu Key Laboratory of Atmospheric Environment Monitoring and Pollution  
Control, Jiangsu Collaborative Innovation Center of Atmospheric Environment and  
Equipment Technology, School of Environmental Science and Engineering, Nanjing  
University of Information Science & Technology, Nanjing 210044, China

<sup>2</sup>State Joint Key Laboratory of Environmental Simulation and Pollution Control,  
College of Environmental Sciences and Engineering, Peking University, Beijing  
100871, China

**Correspondence:** Lei Chen (chenlei@nuist.edu.cn) and Hong Liao  
(hongliao@nuist.edu.cn)

## Abstract

We examined the impacts of aerosol-radiation interactions, including the effects of aerosol-photolysis interaction (API) and aerosol-radiation feedback (ARF), on surface-layer ozone ( $\text{O}_3$ ) concentrations during ~~one-three~~ multi-pollutant air pollution episodes characterized by high  $\text{O}_3$  and  $\text{PM}_{2.5}$  levels ~~from-during~~ 28 July to 3 August 2014 (Episode1), 8-13 July 2015 (Episode2) and 5-11 June 2016 (Episode3) in North China, by using the Weather Research and Forecasting with Chemistry (WRF-Chem) model embedded with an integrated process analysis scheme. Our results show that aerosol-radiation interactions decreased the daytime shortwave radiation at surface by  $92.4\sim 100.3 \text{ W m}^{-2}$  averaged over the complex air pollution areas in these three episodes. The dimming effect reduced the near-surface photolysis rates of  $\text{J}[\text{NO}_2]$  and  $\text{J}[\text{O}^1\text{D}]$  by  $1.8 \times 10^{-3}\sim 2.0 \times 10^{-3} \text{ s}^{-1}$  and  $5.7 \times 10^{-6}\sim 6.3 \times 10^{-6} \text{ s}^{-1}$ , respectively. However, the daytime shortwave radiation in the atmosphere was increased by  $72.8\sim 85.2 \text{ W m}^{-2}$ , which made the atmosphere more stable. The stabilized atmosphere decreased the planetary boundary layer height and 10 m wind speed by  $129.0\sim 249.0 \text{ m}$  and  $0.05\sim 0.12 \text{ m s}^{-1}$ , respectively. The weakened photolysis rates and changed meteorological conditions reduced daytime surface-layer  $\text{O}_3$  concentrations by up to  $9.3\sim 11.4 \text{ ppb}$ , with API and ARF contributing  $74.6\%\sim 90.0\%$  and  $10.0\%\sim 25.4\%$  of the  $\text{O}_3$  decrease in these three episodes, respectively.~~Our results show that aerosol-radiation interactions decrease the daytime downward shortwave radiation at surface, 2 m temperature, 10 m wind speed, planetary boundary layer height, photolysis rates  $\text{J}[\text{NO}_2]$  and  $\text{J}[\text{O}^1\text{D}]$  by  $115.8 \text{ W m}^{-2}$ ,  $0.56^\circ\text{C}$ ,  $0.12 \text{ m s}^{-1}$ ,  $129 \text{ m}$ ,  $1.8 \times 10^{-3} \text{ s}^{-1}$  and  $6.1 \times 10^{-6} \text{ s}^{-1}$ , and increase relative humidity at 2 m and downward shortwave radiation in the atmosphere by  $2.4\%$  and  $72.8 \text{ W m}^{-2}$ . The weakened photolysis rates and changed meteorological conditions reduce surface-layer  $\text{O}_3$  concentrations by up to  $11.4 \text{ ppb}$  ( $13.5\%$ ), with API and ARF contributing  $74.6\%$  and  $25.4\%$  of the  $\text{O}_3$  decrease, respectively. The combined impacts of API and ARF on surface  $\text{O}_3$  are further quantitatively characterized by the ratio of changed  $\text{O}_3$  concentration to local  $\text{PM}_{2.5}$  level. The ratio is calculated to be  $0.14 \text{ ppb} (\mu\text{g m}^{-3})^{-1}$  averaged over the multi-pollutant air pollution area in North China.~~ Process analysis

47 ~~indicates-indicated~~ that the weakened O<sub>3</sub> chemical production ~~makes-made~~ the greatest  
48 contribution to API effect while the reduced vertical mixing ~~is-was~~ the key process for  
49 ARF effect. This study implies that future PM<sub>2.5</sub> reductions will lead to O<sub>3</sub> increases  
50 due to weakened aerosol-radiation interactions. Therefore, tighter controls of O<sub>3</sub>  
51 precursors are needed to offset O<sub>3</sub> increases caused by weakened aerosol-radiation  
52 interactions in the future.

## 1 Introduction

China has been experiencing severe air pollution in recent years, characterized by high loads of PM<sub>2.5</sub> (particulate matter with an aerodynamic equivalent diameter of 2.5 micrometers or less) and high levels of ozone (O<sub>3</sub>). Observational studies exhibited positive correlations and synchronous occurrence of PM<sub>2.5</sub> and O<sub>3</sub> pollution in North China during summer (Zhao et al., 2018; Zhu et al., 2019), indicating that complex air pollution is becoming a major challenge for North China.

Aerosols can absorb and scatter solar radiation ~~and therefore alter~~to affect Earth's energy balance~~radiative balance~~. They can also act as cloud condensation nuclei and ice nuclei, and further modify the microphysical characteristics of clouds (Albrecht et al., 1989; Haywood et al., 2000; Lohmann et al., 2005). Both ways perturb meteorological variables, e.g., temperature, planetary boundary layer height (PBLH), and precipitation, and eventually influence air pollutants (Petäjä et al., 2015; Miao et al., 2018; Zhang et al., 2018). Many studies ~~were~~are focused on the feedback between aerosol and meteorology (Gao et al., 2015; Gao et al., 2016a; Qiu et al., 2017; Chen et al., 2019; Zhu et al., 2021). Gao et al. (2015) used the WRF-Chem model to investigate the feedbacks between aerosols and meteorological variables over the North China Plain in January 2013, and pointed out that aerosols could cause a decrease in surface temperature by 0.8-2.8 °C but an increase of 0.1-0.5 °C around 925 hPa ~~when feedbacks between aerosols and meteorological variables were considered in WRF-Chem model~~. The more stable atmosphere caused by surface cooling and higher-layer heating led to the decreases of surface wind speed and PBLH by 0.3 m s<sup>-1</sup> and 40-200 m, respectively, which further resulted in overall PM<sub>2.5</sub> increases by 10-50 µg m<sup>-3</sup> (2-30%) ~~over Beijing, Tianjin and south Hebei during January 2013~~. By using the same WRF-Chem model, Qiu et al. (2017) reported that the surface downward shortwave radiation and PBLH were reduced by 54.6 W m<sup>-2</sup> and 111.4 m due to aerosol radiative forcing during 21 and 27 February 2014 in the North China Plain. As a result, the surface PM<sub>2.5</sub> concentration averaged over the North China Plain was increased by 34.9 µg m<sup>-3</sup> (20.4%).

Aerosols can also influence O<sub>3</sub> through aerosol-radiation interactions, including



aerosol-photolysis interaction and aerosol-radiation feedback. Aerosols can scatter and absorb UV radiation, and therefore directly affect O<sub>3</sub> photochemistry reactions, which is called aerosol-photolysis interaction (API) (Dickerson et al., 1997; Liao et al., 1999; Li et al., 2011; Lou et al., 2014). The changed meteorological variables due to aerosol radiative forcing can indirectly affect O<sub>3</sub> concentrations, which is called aerosol-radiation feedback (ARF) (Hansen et al., 1997; Gao et al., 2018; Liu et al., 2020). Although the effects of API or ARF on O<sub>3</sub> have been examined by previous studies (Xing et al., 2017; Gao et al., 2018; Gao et al., 2020), the combined effects of API and ARF on O<sub>3</sub>, especially under the conditions of synchronous occurrence of high PM<sub>2.5</sub> and O<sub>3</sub> concentrations, remain largely elusive.

The present study aims to (1) quantify the respective/combined contributions of API and ARF on surface O<sub>3</sub> concentrations by using the WRF-Chem model; (2) explore the prominent physical and/or chemical processes responsible for API and ARF effects by using an integrated process rate (IPR) analysis embedded in WRF-Chem model. In order to draw the general conclusions, three multi-pollutant air pollution episodes characterized by high O<sub>3</sub> and PM<sub>2.5</sub> levels during 28 July to 3 August 2014 (Episode1), 8-13 July 2015 (Episode2) and 5-11 June 2016 (Episode3) in North China are analyzed in this study.~~The analysis is conducted during one multi-pollutant air pollution episode characterized by high O<sub>3</sub> and PM<sub>2.5</sub> levels from 28 July to 3 August 2014 in North China.~~ The model configuration, numerical experiments, observational data, and the integrated process rate analysis are described in section 2. Section 3 shows the model evaluation. The presentation and discussion of the model results are exhibited in section 4, and the conclusions s and discussions are ~~is~~ provided in section 5.

## 2 Methods

### 2.1 Model configuration

The version 3.7.1 of the online-coupled Weather Research and Forecasting with Chemistry (WRF-Chem) model (Grell et al., 2005; Skamarock et al., 2008) is used in this study to explore the impacts of aerosol-radiation interactions on surface-layer O<sub>3</sub> in North China. WRF-Chem can simulate gas phase species and aerosols coupled with

meteorological fields, and has been widely used to investigate air pollution over North China (Gao et al., 2016a; Gao et al., 2020; Wu et al., 2020). As shown in Fig. 1, we design two nested model domains with the number of grid points of 57 (west–east) × 41 (south–north) and 37 (west–east) × 43 (south–north) at 27 and 9 km horizontal resolutions, respectively. The parent domain centers at (39 °N, 117 °E). The model contains 29 vertical levels from the surface to 50 hPa, with 14 levels below 2 km for the fully description of the vertical structure of planetary boundary layer (PBL).

The Carbon Bond Mechanism Z (CBM-Z) is selected as the gas-phase chemical mechanism (Zaveri and Peters, 1999), and the full 8-bin MOSAIC (Model for Simulating Aerosol Interactions and Chemistry) aerosol module with aqueous chemistry is used to simulate aerosol evolution (Zaveri et al., 2008). The photolysis rates are calculated by the Fast-J scheme (Wild et al., 2000). Other major physical parameterizations used in this study are listed in Table 1.

The initial and boundary meteorological conditions are provided by the National Centers for Environmental Prediction (NCEP) Final Analysis data with a spatial resolution of  $1^{\circ} \times 1^{\circ}$ . In order to limit the model bias of simulated meteorological fields, the four-dimensional data assimilation (FDDA) is used with ~~a~~-the nudging coefficient of  $3.0 \times 10^{-4}$  for ~~the~~-wind, temperature and humidity (no analysis nudging is applied for the inner domain) (Lo et al., 2008; Otte, 2008). Chemical initial and boundary conditions are obtained from the Model for Ozone and Related chemical Tracers, version 4 (MOZART-4) forecasts (Emmons et al., 2010).

Anthropogenic emissions in Episode1 are taken from the 2010 MIX Asian emission inventory, and the Multi-resolution Emission Inventory for China (MEIC) is used in Episode2 and Episode3 (<http://www.meicmodel.org/>)~~Anthropogenic emissions are taken from the 2010 MIX Asian emission inventory~~ (Li et al., 2017a), These emission inventories~~which~~ provides emissions of sulfur dioxide (SO<sub>2</sub>), nitrogen oxides (NO<sub>x</sub>), carbon monoxide (CO), non-methane volatile organic compounds (NMVOCs), carbon dioxide (CO<sub>2</sub>), ammonia (NH<sub>3</sub>), black carbon (BC), organic carbon (OC), PM<sub>10</sub> (particulate matter with aerodynamic diameter is 10 μm and less) and PM<sub>2.5</sub>. Emissions are aggregated from four sectors, including power generation, industry, residential, and

transportation, with  $0.25^\circ \times 0.25^\circ$  spatial resolution. Biogenic emissions are calculated online by the Model of Emissions of Gases and Aerosols from Nature (MEGAN) (Guenther et al., 2006).

## 2.2 Numerical experiments

To quantify the impacts of API and ARF on  $O_3$ , three case simulations have been conducted: (1) BASE – the base simulation coupled with the interactions between aerosol and radiation, which includes both impacts of API and ARF; (2) NOAPI – the same as the BASE case, but the impact of API is turned off (aerosol optical properties are set to zero in the photolysis module), following Wu et al. (2020); (3) NOALL – both the impacts of API and ARF are turned off (removing the mass of aerosol species when calculating aerosol optical properties in the optical module), following Qiu et al. (2017). The differences between BASE and NOAPI (i.e., BASE minus NOAPI) represent the impacts of API. The contributions from ARF can be obtained by comparing NOAPI and NOALL (i.e., NOAPI minus NOALL). The combined effects of API and ARF on  $O_3$  concentrations can be quantitatively evaluated by the differences between BASE and NOALL (i.e., BASE minus NOALL).

All the experiments in Episode1, Episode2 and Episode3 are conducted from 26 July to 3 August 2014, 6-13 July 2015 and 3-11 June 2016, respectively, with the first 40 hours as the model spin-up in each case. Simulation results from the BASE cases of the three episodes are used to evaluate the model performance.~~Each simulation is conducted from 26 July to 3 August 2014, with the first 40 hours as the model spin-up. Simulation results from the BASE case during 28 July and 3 August 2014 are used to evaluate the model performance.~~

## 2.3 Observational data

Simulation results are compared with meteorological and chemical measurements. The surface-layer meteorological data (2 m temperature ( $T_2$ ), 2 m relative humidity ( $RH_2$ ), and 10 m wind speed ( $WS_{10}$ )), with ~~a~~the temporal resolution of 3 h, at ~~three~~ten stations (Table S1) are obtained from NOAA's National Climatic Data Center (<https://gis.ncdc.noaa.gov/maps/ncei/cdo/hourly>). The radiosonde data of temperature

at 08:00 and 20:00 LST in Beijing ([39.93 °N, 116.28 °E](#)) are provided by the University of Wyoming (<http://weather.uwyo.edu/>). Observed hourly concentrations of PM<sub>2.5</sub> and O<sub>3</sub> at thirty-two sites (Table S2) in North China are collected from the China National Environmental Monitoring Center (CNEMC). The photolysis rate of nitrogen dioxide ( $\text{NO}_2$ ) ( $J[\text{NO}_2]$ ) measured at the Peking University site (39.99 °N, 116.31 °E) is also used to evaluate the model performance. More details about the measurement technique of  $J[\text{NO}_2]$  can be found in Wang et al. (2019). [The aerosol optical depth \(AOD\) at Beijing site \(39.98°N, 116.38°E\) is provided by AERONET \(level 2.0, http://aeronet.gsfc.nasa.gov/\). The AOD at 675 nm and 440 nm are used to derive the AOD at 550 nm to compare with the simulated ones.](#)

## 2.4 Integrated process rate analysis

Integrated process rate (IPR) analysis has been widely used to quantify the contributions of different processes to O<sub>3</sub> variations (Goncalves et al., 2009; Gao et al., 2016b; Tang et al., 2017; Gao et al., 2018). In this study, four physical/chemical processes are considered, including vertical mixing (VMIX), net chemical production (CHEM), horizontal advection (ADVH), and vertical advection (ADVZ). VMIX is initiated by turbulent process and closely related to PBL development, which influences O<sub>3</sub> vertical gradients. CHEM represents the net O<sub>3</sub> chemical production (chemical production minus chemical consumption). ADVH and ADVZ represent transport by winds (Gao et al., 2016b). In this study, we define ADV as the sum of ADVH and ADVZ.

## 3 Model evaluation

Reasonable representation of observed meteorological and chemical variables by the WRF-Chem model can provide foundation for evaluating the impacts of aerosols on surface-layer ozone concentrations. The model results presented in this section are taken from the BASE cases [in the three episodes](#). The concentrations of air pollutants are averaged over the thirty-two observation sites in Beijing, Tianjin and Baoding. To ensure the data quality, the mean value for each time is calculated only when concentrations are available at more than sixteen sites, [as did in Li et al. \(2019a\)](#).

### 3.1 Chemical simulations

Figure 2 shows the ~~spatial~~-temporal variations of observed and simulated PM<sub>2.5</sub> and O<sub>3</sub> concentrations over North China ~~for the three episodes during 28 July to 3 August 2014. The observed higher concentrations in Beijing and Baoding than those in Tianjin are well reproduced by the WRF-Chem model. As shown in Fig. 2, the temporal variations of observed PM<sub>2.5</sub> can be well performed by the model with correlation coefficients (R) of 0.66, 0.56 and 0.73 and normalized mean bias (NMB) of -19.2%, -3.9% and 30.4% during Episode1, Episode2 and Episode3, respectively. The model also tracks well the diurnal variation of O<sub>3</sub> over the North China, with R of 0.86, 0.91 and 0.86 and NMB of -12.0%, 0.4% and 1.6% for Episode1, Episode2 and Episode3, respectively. The model can also reasonably capture the temporal variations of observed PM<sub>2.5</sub> and O<sub>3</sub> with high correlation coefficients (R) of 0.66 for PM<sub>2.5</sub> and 0.86 for O<sub>3</sub>, although simulated results underestimate the observed PM<sub>2.5</sub> by -19.2% and O<sub>3</sub> by -12.0%. The failure to reproduce PM<sub>2.5</sub> peak values may be attributed to incomplete treatments of chemical reactions in WRF-Chem, e.g., the aqueous-phase reactions of SO<sub>2</sub> oxidized by NO<sub>2</sub> in aerosol water (Cheng et al., 2016). More statistical parameters between simulations and observations are presented in Table 2.~~

~~Figure S1 shows the correlation between observed and simulated AOD at 550 nm in Beijing. In the WRF-Chem model, the AOD at 550 nm are calculated by using the values at 400 and 600 nm according to the Angstrom exponent. Analyzing Fig. S1, the model can reproduce the observed AOD with R of 0.7 and NMB of 7.9%.~~

### 3.2 Meteorological simulations

Figure 3 shows the time series of observed and simulated ~~T<sub>2</sub>, RH<sub>2</sub>, WS<sub>10</sub> and J[NO<sub>2</sub>]~~ during the three episodes. The observed T<sub>2</sub>, RH<sub>2</sub>, WS<sub>10</sub> are averaged over the ten meteorological observation stations, and the J[NO<sub>2</sub>] are measured at Peking University. Most of the monitored J[NO<sub>2</sub>] in Episode3 are unavailable, so the comparison of J[NO<sub>2</sub>] in Episode3 is not shown. ~~T<sub>2</sub>, RH<sub>2</sub>, and WS<sub>10</sub> averaged over three cities (Beijing, Tianjin, and Baoding), and J[NO<sub>2</sub>] at Peking University during 28 July to 3 August 2014. The statistical metrics for T<sub>2</sub>, RH<sub>2</sub>, WS<sub>10</sub>, and J[NO<sub>2</sub>] are also presented in Table 2.~~

Generally, the model can depict the temporal variations of  $T_2$  fairly well with R of 0.98 and the mean bias (MB) of  $-1.9 \sim -0.9 \sim -0.2$  °C. For  $RH_2$ , the R and MB are  $0.91 \sim 0.97 \sim 0.93$  and  $-4.0\% \sim -1.9\% \sim -6.0\%$ , respectively. Although WRF-Chem model overestimates  $WS_{10}$  with the MB of  $0.6 \sim 0.90 \sim 0.6$  m s<sup>-1</sup>, the R for  $WS_{10}$  is  $0.70 \sim 0.89 \sim 0.70$  and the root-mean-square error (RMSE) is  $0.9 \sim 1.54 \sim 0$  m s<sup>-1</sup>, which is smaller than the threshold of model performance criteria (2 m s<sup>-1</sup>) proposed by Emery et al. (2001). The ~~large~~ positive bias in wind speed ~~was can~~ also ~~be reproduced reported~~ in other studies (Zhang et al., 2010; Gao et al., 2015; Liao et al., 2015; Qiu et al., 2017). The predicted J[NO<sub>2</sub>] agrees well with the observations with R of 0.97  $\sim 0.98$  and NMB of 6.8%  $\sim 6.9\%$ . We also conduct comparisons ~~of between~~ observed and simulated temperature profiles at 08:00 and 20:00 LST in Beijing during ~~the three episodes (Fig. S2) 29 July to 1 August 2014 in Figure S1~~. The vertical profiles of observed temperature ~~can be, especially the thermal inversion layer occurred on 31 July around 1600 m, is~~ well captured by the model ~~in these three complex air pollution episodes~~. Generally, the WRF-Chem model ~~can~~ reasonably reproduces the temporal variations of observed meteorological parameters.

## 4 Results

It is known that co-occurrence of PM<sub>2.5</sub> and O<sub>3</sub> pollution is frequently observed nowadays over China (Dai et al., 2021). The complex air pollution characterized by high PM<sub>2.5</sub> and O<sub>3</sub> levels has already received widespread ~~attentions~~ attention from both scientists and policy-makers. Therefore, we examine the impacts of aerosol-radiation interactions on O<sub>3</sub> concentrations with a special focus on the complex air pollution areas (CAPAs, Fig. ~~S2S3~~) in the three episodes, where the mean simulated daily PM<sub>2.5</sub> and MDA8 (maximum daily 8-h average) O<sub>3</sub> concentrations are larger than 75 µg m<sup>-3</sup> and 80 ppb, respectively, based on the National Ambient Air Quality Standards (<http://www.mee.gov.cn>).

### 4.1 Impacts of aerosol-radiation interactions on meteorology

Figure 4 shows the impacts of aerosol-radiation interactions on ~~downward~~ shortwave radiation at the surface (BOT\_SW), ~~downward~~ shortwave radiation in the atmosphere (ATM\_SW), PBLH, ~~T<sub>2</sub>, RH<sub>2</sub>~~, and  $WS_{10}$  during the daytime (08:00-17:00

LST) from Episode1 to Episode328 July to 3 August 2014. Analyzing the As a results of the interactions between aerosol and radiation (the combined impacts of API and ARF), BOT\_SW is decreased over the entire simulated domain in the three episodes. ~~Over CAPAs, the BOT\_SW is decreased by~~ with the decreases of 93.2 W m<sup>-2</sup> (20.5%), 100.3 W m<sup>-2</sup> (19.5%) and 92.4 W m<sup>-2</sup> (19.2%) over CAPAs, respectively ~~115.8 W m<sup>-2</sup> (20.5%)~~. Contrary to the changes in BOT\_SW, ATM\_SW is increased significantly in the three episodes with ~~an~~ the increases of 72.8 W m<sup>-2</sup> (25.3%), 85.2 W m<sup>-2</sup> (29.0%) and 73.7 W m<sup>-2</sup> (26.4%) over CAPAs, respectively. The decreased BOT\_SW perturbs the near-surface energy flux, which weakens convection and suppresses the development of PBL (Li et al., 2017b). The mean PBLHs ~~averaged over CAPAs is calculated to decrease~~ are decreased by 129.0 m (13.0%), 249.0 m (20.9%) and 224.6 m (19.0%), respectively. ~~The reduced surface radiation budget can directly lead to changes in near-surface temperature. Therefore, the changes in T<sub>2</sub> have the similar spatial patterns with BOT\_SW; the surface temperature is decreased by 0.56 °C averaged over CAPAs. RH<sub>2</sub> is increased over most of the domain with an average rise of 2.4%, which is beneficial for the hygroscopic growth of aerosols.~~ WS<sub>10</sub> exhibits overall reductions over CAPAs and is calculated to decrease by 0.12 m s<sup>-1</sup> (3.6%), 0.05 m s<sup>-1</sup> (1.6%), and 0.12 m s<sup>-1</sup> (3.0%) for the three episodes, respectively ~~on average~~. We also examine the changed meteorological variables caused by API and ARF respectively. As shown in Fig. ~~S3S4 and S5~~, API has little impact on meteorological variables; which means the major contributor to the meteorology variability is ARF, ~~the above changes are mainly caused by ARF~~.

## 4.2 Impacts of aerosol-radiation interactions on photolysis

Figure 5 shows the spatial distributions of mean daytime surface-layer PM<sub>2.5</sub> concentrations simulated by BASE cases and the changes in J[NO<sub>2</sub>] and J[O<sup>1</sup>D] due to aerosol-radiation interactions from Episode1 to Episode328 July to 3 August 2014. When the combined impacts (API and ARF) are considered, J[NO<sub>2</sub>] and J[O<sup>1</sup>D] are decreased over the entire domain in the three episodes, and; the spatial patterns of changed J[NO<sub>2</sub>] and J[O<sup>1</sup>D] are similar to that of simulated PM<sub>2.5</sub>. Analyzing the three



simulated episodes, the surface  $J[\text{NO}_2]$  averaged over CAPAs are decreased by  $1.8 \times 10^{-3} \text{ s}^{-1}$  (40.5%),  $2.0 \times 10^{-3} \text{ s}^{-1}$  (36.8%) and  $1.8 \times 10^{-3} \text{ s}^{-1}$  (36.0%), respectively. The decreased surface  $J[\text{O}^1\text{D}]$  over CAPAs are  $6.1 \times 10^{-6} \text{ s}^{-1}$  (48.8%),  $6.3 \times 10^{-6} \text{ s}^{-1}$  (41.4%) and  $5.7 \times 10^{-6} \text{ s}^{-1}$  (44.6%), respectively. The surface  $J[\text{NO}_2]$  and  $J[\text{O}^1\text{D}]$  are decreased by  $1.8 \times 10^{-3} \text{ s}^{-1}$  (40.5%) and  $6.1 \times 10^{-6} \text{ s}^{-1}$  (48.8%) averaged over CAPAs. Figure S4 S6 exhibits the impacts of API and ARF on surface  $J[\text{NO}_2]$  and  $J[\text{O}^1\text{D}]$  percentage changes in surface  $J[\text{NO}_2]$  and  $J[\text{O}^1\text{D}]$  caused by API and ARF respectively. Conclusions can be summarized It is found that  $J[\text{NO}_2]$  and  $J[\text{O}^1\text{D}]$  are significantly modified by API and little affected by ARF.

### 4.3 Impacts of aerosol-radiation interactions on $\text{O}_3$

Figure 6 shows the changes in surface-layer  $\text{O}_3$  due to API, ARF, and the combined effects (denoted as ALL) from Episode1 to Episode3. As shown in Fig. 6(a1-a3) Fig. 6a, API alone leads to overall surface  $\text{O}_3$  decreases over the entire domain with an average reductions of 8.5 ppb (10.1%), 9.0 ppb (10.6%) and 8.3 ppb (10.4%) over CAPAs in the three episodes, respectively. The changes can be explained by the substantially diminished UV radiation due to aerosol loading, which significantly weakens the efficiency of photochemical reactions and restrains  $\text{O}_3$  formation. However, the decreased surface  $\text{O}_3$  concentrations due to ARF, however, is are only 2.9 ppb (3.1%, Fig. 6(b1)), 1.0 ppb (1.2%, Fig. 6(b2)) and 1.0 ppb (1.1%, Fig. 6(b3)) for the three episodes, which indicates that API is the dominant way for  $\text{O}_3$  reduction related to aerosol-radiation interactions. The distributions of changed  $\text{O}_3$  concentrations coincide with  $\text{NO}_x$  variations (Fig. S5b). Since North China is VOC-limited (Jin et al., 2015), the increase in  $\text{NO}_x$  due to ARF may partly explain the  $\text{O}_3$  decrease. Fig. 6(c1-c3) presents the combined effects of API and ARF are shown in Fig. 6e. Generally, aerosol-radiation interactions decrease the surface  $\text{O}_3$  concentrations by 11.4 ppb (13.5%), 10.0 ppb (11.9%) and 9.3 ppb (11.6%) averaged over CAPAs in the three episodes, respectively.

We further define an index to characterize the effects of aerosols on surface  $\text{O}_3$  concentrations. The ratio of changes in  $\text{O}_3$  to local  $\text{PM}_{2.5}$  levels is defined as:



$$ROP = \frac{\Delta O_3}{PM_{2.5\_BASE}},$$

where  $\Delta O_3$  is the changed  $O_3$  concentration caused by ALL, and  $PM_{2.5\_BASE}$  is the surface  $PM_{2.5}$  concentration simulated in the BASE scenario. The calculated ROP is  $0.14 \text{ ppb } (\mu\text{g m}^{-3})^{-1}$  averaged over CAPAs, which means when the concentrations of  $PM_{2.5}$  is  $100 \mu\text{g m}^{-3}$ , the  $O_3$  decrease will be up to 14 ppb over CAPAs due to aerosol-radiation interactions.

#### 4.4 Influencing mechanism of aerosol-radiation interactions on $O_3$

Figure 7a shows mean results of the three episodes (Episode1, Episode2 and Episode3) in diurnal variations of simulated daytime surface-layer  $O_3$  concentrations from BASE, NOAPI and NOALL cases averaged over CAPAs. ~~diurnal variations of simulated surface daytime  $O_3$  concentrations over CAPAs in three cases (BASE, NOAPI, and NOALL).~~ All the experiments (BASE, NOAPI and NOALL) ~~eases~~ present  $O_3$  increases from 08:00 LST. It is shown that the simulated  $O_3$  concentrations in BASE case increase more slowly than that in NOAPI and NOALL cases. To explain the underlying mechanisms of API and ARF impacts on  $O_3$ , we quantify the variations in contributions of different processes (ADV, CHEM, and VMIX) to  $O_3$  by using the IPR analysis.

Figure 7b shows hourly surface  $O_3$  changes induced by each physical/chemical process (i.e., ADV, CHEM, and VMIX) in BASE case averaged from Episode1 to Episode3. The significant positive contribution to the hourly variation in  $O_3$  is contributed by VMIX, and the contribution reaches the maximum at about ~~1009:00~~ 09:00 LST. ~~After 14:00 LST, the contribution from VMIX remains constant (nearly  $+2 \text{ ppb h}^{-1}$ ), which is probably attributed to the stable boundary layer development (Tang et al., 2016).~~ The CHEM process makes negative contributions at around 09:00 and 16:00 LST, which means that the chemical consumption of  $O_3$  is stronger than the chemical production. At noon, the net chemical contribution turns to be positive due to stronger solar UV radiation. The contribution from all the processes (NET, the sum of VMIX, CHEM, and ADV) to  $O_3$  variation is peaked at the noon and then becomes weakened. After sunset (17:00 LST), the NET contribution turns to be negative over CAPAs,

leading to O<sub>3</sub> decrease.

Figure 7c shows the changes in hourly process contributions caused by API averaged from Episode1 to Episode3. The chemical production of O<sub>3</sub> is suppressed significantly due to aerosol impacts on photolysis rates. The weakened O<sub>3</sub> chemical production decreases the contribution from CHEM, and results in a negative value of CHEM\_DIF (~~-3.53.2~~ ppb h<sup>-1</sup>). In contrast to CHEM\_DIF, the contribution from changed VMIX (VMIX\_DIF) to O<sub>3</sub> concentration due to API is always positive, and the mean value is +~~3.13.0~~ ppb h<sup>-1</sup>. The impact of API on ADV process is relatively small (~~-0.360.26~~ ppb h<sup>-1</sup>). NET\_DIF, namely the sum of VMIX\_DIF, CHEM\_DIF and ADV\_DIF, indicates the differences in hourly O<sub>3</sub> changes caused by API. As shown in Fig. 7c, NET\_DIF is almost negative during the daytime over CAPAs with the mean value of ~~-0.760.46~~ ppb h<sup>-1</sup>. This is because the decreases in CHEM and ADV are larger than the increases in VMIX caused by API; the O<sub>3</sub> decrease is mainly attributed to the significantly decreased contribution from CHEM. The maximum difference in O<sub>3</sub> between BASE and NOAPI appears at ~~1711~~:00 LST with a value of ~~-10.111.1~~ ppb (Fig. 7a).

Figure 7d shows the impacts of ARF on each physical/chemical process contribution to the hourly O<sub>3</sub> variation averaged from Episode1 to Episode3. At 08:00 LST, the change in VMIX due to ARF is large with a value of ~~-4.63.5~~ ppb h<sup>-1</sup>, resulting in a net negative variation with all processes considered. The decrease in O<sub>3</sub> reaches the maximum with the value of ~~6.15.2~~ ppb at around ~~0908~~:00 LST over CAPAs (Fig. 7a). During ~~1009~~:00 to 16:00 LST, the positive VMIX\_DIF (mean value of +~~0.590.20~~ ppb h<sup>-1</sup>) or the positive CHEM\_DIF (mean value of +~~0.160.55~~ ppb h<sup>-1</sup>) is the major process to positive NET\_DIF.

When both impacts of API and ARF are considered, the variation pattern of the difference in hourly process contribution shown in Fig. 7e is similar to that in Fig. 7c, which indicates that API is the dominant factor to surface-layer O<sub>3</sub> reduction.

Figure 8 presents the vertical profiles of simulated daytime O<sub>3</sub> concentrations in three cases (BASE, NOAPI, and NOALL), and the differences in contributions from each physical/chemical process to hourly O<sub>3</sub> variations caused by API, ARF and the

combined effects ~~averaged over CAPAs from Episode1 to Episode3 during 28 July to 3 August 2014 over CAPAs~~. As shown in Fig. 8a, the O<sub>3</sub> concentration is lower in BASE than that in other two scenarios (NOAPI and NOALL), especially at the lower 12 levels ~~(below 863.0 m)~~, owing to the impacts of aerosols (API and/or ARF).

The changes in each process contribution caused by API are presented in Fig. 8b. The contribution from CHEM\_DIF is ~~-2.142.0~~ ppb h<sup>-1</sup> for ~~the~~ first seven layers ~~(from 27.6 to 342.8 m)~~. Conversely, the contribution from VMIX\_DIF shows a positive value ~~under the 342.8 m (between the first layer to the seventh layer) at the lower seven layers~~ with the mean value of +1.7 ppb h<sup>-1</sup>. The positive variation in VMIX due to API may be associated with the different vertical gradient of O<sub>3</sub> between BASE and NOAPI ~~eases~~. The contributions of changed advections (ADVH\_DIF and ADVZ\_DIF) are relatively small, with mean values of ~~+0.250.07~~ and ~~-0.470.21~~ ppb h<sup>-1</sup> ~~respectively~~ below the first seven layers, which may result from small impact of API on wind filed (Fig. ~~S3a~~~~S5(a4-c4)~~). The net difference is a negative value (~~-0.660.44~~ ppb h<sup>-1</sup>); API leads to O<sub>3</sub> reduction not only nearly surface but also ~~in the~~ aloft.

Figure 8c shows the differences in O<sub>3</sub> budget due to ARF. When the ARF is considered, the vertical turbulence is weakened and the development of PBL is inhibited, which makes VMIX\_DIF negative at the lower ~~7-seven~~ layers ~~(below the 342.8 m)~~ with a mean value of ~~-0.550.64~~ ppb h<sup>-1</sup>, but the variation in CHEM caused by ARF is positive with a mean value of ~~+0.60.72~~ ppb h<sup>-1</sup>. ~~The chemical production of tropospheric O<sub>3</sub> is affected by both photolysis rate and the concentrations of precursors (Tie et al., 2009).~~ The enhanced O<sub>3</sub> precursors due to ARF can promote the chemical production of O<sub>3</sub> ~~(Tie et al., 2009; Gao et al., 2018)~~. The changes of ADVZ and ADVH (ADVZ\_DIF and ADVH\_DIF) caused by ARF are associated with the variations in wind filed. When ARF is considered, the horizontal wind speed is decreased (Fig. ~~S7(a)~~~~6a~~), which makes ADVH\_DIF positive at the lower twelve layers with a mean value of ~~+0.50.25~~ ppb h<sup>-1</sup>. However, ADVZ\_DIF is negative at these layers with a mean value of ~~-0.480.27~~ ppb h<sup>-1</sup> because aerosol radiative effects decrease the transport of O<sub>3</sub> from the upper to lower layers (Fig. ~~S6b~~~~S7(b)~~).

In Fig. 8d, the pattern and magnitude of the differences in process contributions between BASE and NOALL are similar to those caused by API, indicating ~~again~~ the dominate ~~contributor role~~ of API on O<sub>3</sub> changes. The impacts of API on O<sub>3</sub> both near the surface and aloft are greater than those of ARF.

Figure S8 and S9 detailed show the influencing mechanism of aerosol-radiation interactions on O<sub>3</sub> in each episode. Similar variation characteristics can be found among the three episodes as the mean situation discussed above, with the larger impacts of API on O<sub>3</sub> both near the surface and aloft than those of ARF, indicating the major contributor of API on O<sub>3</sub> reduction related with aerosol-radiation interactions.

## 5 Conclusions and Discussions

In this study, the fully coupled regional chemistry transport model WRF-Chem is applied to investigate the impacts of aerosol-radiation interactions, including the impacts of aerosol-photolysis interaction (API) and the impact of aerosol-radiation feedback (ARF), on O<sub>3</sub> during ~~a~~ summertime complex air pollution episodes from 28 July to 3 August 2014 (Episode1), 8-13 July 2015 (Episode2) and 5-11 June 2016 (Episode3). Three sensitivity experiments are designed to quantify the respective and combined impacts from API and ARF. Generally, the spatiotemporal distributions of observed pollutant concentrations and meteorological parameters ~~can beare~~ captured fairly well by the model with ~~high~~ correlation coefficients of 0.56~0.91~~0.66~0.86~~ for pollutant concentrations and 0.70~0.98 for meteorological parameters.

Sensitivity experiments show that aerosol-radiation interactions decrease BOT\_SW, ~~T<sub>25</sub>~~WS<sub>10</sub>, PBLH, J[NO<sub>2</sub>], and J[O<sup>1</sup>D] by 92.4~100.3 W m<sup>-2</sup>, 0.05~0.12 m s<sup>-1</sup>, 129.0~249.0 m, 1.8 × 10<sup>-3</sup>~2.0 × 10<sup>-3</sup> s<sup>-1</sup>, and 5.7 × 10<sup>-6</sup>~6.3 × 10<sup>-6</sup>~~115.8 W m<sup>-2</sup>, 0.56 °C, 0.12 m s<sup>-1</sup>, 129 m, 1.8 × 10<sup>-3</sup> s<sup>-1</sup>, and 6.1 × 10<sup>-6</sup> s<sup>-1</sup>~~ over CAPAs, and increase ATM\_SW ~~and RH<sub>2</sub>~~ by 72.8~85.2 W m<sup>-2</sup>~~and 2.4%~~. The changed meteorological variables and weakened photochemistry reaction further reduce surface-layer O<sub>3</sub> concentrations by up to 9.3~11.4 ppb~~(13.5%)~~, with API and ARF contributing 74.6%~90.0% and 10.0%~25.4%, respectively. ~~The combined impacts of API and ARF on O<sub>3</sub> can be characterized by the ratio of changed O<sub>3</sub> (ΔO<sub>3</sub>) to local PM<sub>2.5</sub> level~~

( $\text{PM}_{2.5\_}\text{BASE}$ ), defining as  $\text{ROP} = \Delta\text{O}_3 / \text{PM}_{2.5\_}\text{BASE}$ . The calculated ROP is  $-0.14 \text{ ppb} (\mu\text{g m}^{-3})^{-1}$  averaged over CAPAs.

We further examine the influencing mechanism of aerosol-radiation interactions on  $\text{O}_3$  by using integrated process rate analysis. API can directly affect  $\text{O}_3$  by reducing the photochemistry reactions within the lower several hundred meters and therefore amplify the  $\text{O}_3$  vertical gradient, which promotes ~~the contribution from VMIX and the~~ vertical mixing of  $\text{O}_3$ . The reduced photochemistry reactions of  $\text{O}_3$  weaken the chemical contribution and reduce surface  $\text{O}_3$  concentrations, even though the enhanced vertical mixing can partly counteract the reduction. ARF affects  $\text{O}_3$  concentrations indirectly through the changed meteorological variables, e.g., the decreased PBLH. The suppressed PBL can weaken the vertical mixing of  $\text{O}_3$  by turbulence. Generally, the impacts of API on  $\text{O}_3$  both near the surface and aloft are greater than those of ARF, indicating the dominant role of API on  $\text{O}_3$  reduction related with aerosol-radiation interactions.

This study provides a detailed understanding of aerosol impacts on  $\text{O}_3$  through aerosol-radiation interactions (including both API and ARF). The results imply that future  $\text{PM}_{2.5}$  reductions will lead to  $\text{O}_3$  increases due to weakened aerosol-radiation interactions. ~~A recent study~~Recent study emphasized the need for controlling VOCs emissions to mitigate  $\text{O}_3$  pollution (Li et al., 2019b). Therefore, tighter controls of  $\text{O}_3$  precursors (especially VOCs emissions) are needed to counteract future  $\text{O}_3$  increases caused by weakened aerosol-radiation interactions, ~~and the contributions of different~~ mitigation strategies with the impacts of aerosol-radiation interactions to  $\text{O}_3$  air quality will be discussed detailedly in our future work.

There are some limitations to this work. The uncertainty of the lack of secondary organic aerosols (SOA), and the missing mechanisms of some heterogeneous reactions may result in large uncertainties in the final simulation results. Gao et al. (2017) added some SOA formation mechanisms into the MOSAIC module by using the volatility basis set (VBS) in WRF-Chem and found that the surface  $\text{PM}_{2.5}$  concentrations in urban Beijing were reduced by  $1.9 \mu\text{g m}^{-3}$  due to the weakened ARF effect during Asia-Pacific Economic Cooperation (APEC). Similar magnitude can also be found in Zhou et al.

(2019) ( $-1.8 \mu\text{g m}^{-3}$ ) who did not consider the impacts of SOA in WRF-Chem when analyzing the impacts of weakened ARF on  $\text{PM}_{2.5}$  during APEC. Therefore, more work should be conducted to explore the impacts of ARF on  $\text{PM}_{2.5}$  and  $\text{O}_3$  concentrations under consideration of SOA in future.

## **Data availability**

The observed hourly surface concentrations of air pollutants are derived from the China National Environmental Monitoring Center (<http://www.cnemc.cn>). The observed surface meteorological data are obtained from NOAA's National Climatic Data Center (<https://gis.ncdc.noaa.gov/maps/ncei/cdo/hourly>). The radiosonde data are provided by the University of Wyoming (<http://weather.uwyo.edu/>). The photolysis rates of nitrogen dioxide in Beijing are provided by Xin Li ([li\\_xin@pku.edu.cn](mailto:li_xin@pku.edu.cn)). The aerosol optical depth in Beijing is obtained from the AERONET level 2.0 data collection (<http://aeronet.gsfc.nasa.gov/>). The simulation results can be accessed by contacting Lei Chen ([chenlei@nuist.edu.cn](mailto:chenlei@nuist.edu.cn)) and Hong Liao ([hongliao@nuist.edu.cn](mailto:hongliao@nuist.edu.cn)).

## **Author contributions**

HY, LC, and HL conceived the study and designed the experiments. HY and LC performed the simulations and carried out the data analysis. JZ, WW, and XL provided useful comments on the paper. HY prepared the paper with contributions from all co-authors.

## **Competing interests**

The authors declare that they have no competing interests.

## **Acknowledgements**

This work is supported by the National Key R&D Program of China (2019YFA0606804), the National Natural Science Foundation of China (42007195), ~~and~~ the Meteorological Soft Science Program of China Meteorological Administration (2021ZZXM46), and the Postgraduate Research and Practice Innovation Program of Jiangsu Province (KYCX21\_1014). We acknowledge the High Performance Computing Center of Nanjing University of Information Science & Technology for their support of this work.

## Reference

- Albrecht, B. A.: Aerosols, cloud microphysics, and fractional cloudiness, *Science*, 245, 1227–1230, 1989.
- Chen, F. and Dudhia, J.: Coupling an Advanced Land Surface – Hydrology Model with the Penn State – NCAR MM5 Modeling System. Part I: Model Implementation and Sensitivity, *Mon. Weather Rev.*, 129(4), 569–585, 2001.
- Chen, L., Zhu, J., Liao, H., Gao, Y., Qiu, Y., Zhang, M., Liu, Z., Li, N., and Wang, Y.: Assessing the formation and evolution mechanisms of severe haze pollution in the Beijing–Tianjin–Hebei region using process analysis, *Atmos. Chem. Phys.*, 19, 10845–10864, <https://doi.org/10.5194/acp-19-10845-2019>, 2019.
- ~~Cheng, Y., Zheng, G., Chao, W., Mu, Q., Bo, Z., Wang, Z., Meng, G., Qiang, Z., He, K., and Carmichael, G.: Reactive nitrogen chemistry in aerosol water as a source of sulfate during haze events in China, *Science Advances*, 2, <https://doi.org/10.1126/sciadv.1601530>, 2016.~~
- Dai, H., Zhu, J., Liao, H., Li, J., Liang, M., Yang, Y., and Yue, X.: Co-occurrence of ozone and PM<sub>2.5</sub> pollution in the Yangtze River Delta over 2013–2019: Spatiotemporal distribution and meteorological conditions, *Atmos. Res.*, 249, 105363, 2021.
- Dickerson, R. R., Kondragunta, S., Stenchikov, G., Civerolo, K. L., Doddridge, B. G., and Holben, B. N.: The impact of aerosols on solar ultraviolet radiation and photochemical smog, *Science*, 278, 827–830, [10.1126/science.278.5339.827](https://doi.org/10.1126/science.278.5339.827), 1997.
- Emery, C., Tai, E., and Yarwood, G.: Enhanced meteorological modeling and performance evaluation for two Texas ozone episodes, in: Prepared for the Texas Natural Resource Conservation Commission, ENVIRON International Corporation, Novato, CA, USA, 2001.
- Emmons, L. K., Walters, S., Hess, P. G., Lamarque, J.-F., Pfister, G. G., Fillmore, D., Granier, C., Guenther, A., Kinnison, D., Laepple, T., Orlando, J., Tie, X., Tyndall, G., Wiedinmyer, C., Baughcum, S. L., and Kloster, S.: Description and evaluation of the Model for Ozone and Related chemical Tracers, version 4 (MOZART-4), *Geosci.*



Model Dev., 3, 43–67, doi:10.5194/gmd-3-43-2010, 2010.

Foken, T.: 50 years of the Monin-Obukhov similarity theory, Bound.-Layer Meteor., 119, 431–437, 2006.

Gao, J., Li, Y., Zhu, B., Hu, B., Wang, L., and Bao, F.: What have we missed when studying the impact of aerosols on surface ozone via changing photolysis rates?, Atmos. Chem. Phys., 20, 10831–10844, <https://doi.org/10.5194/acp-20-10831-2020>, 2020.

Gao, J. H., Zhu, B., Xiao, H., Kang, H. Q., Pan, C., Wang, D. D., and Wang, H. L.: Effects of black carbon and boundary layer interaction on surface ozone in Nanjing, China, Atmos. Chem. Phys., 18, 7081–7094, <https://doi.org/10.5194/acp-18-7081-2018>, 2018.

Gao, M., Carmichael, G. R., Wang, Y., Saide, P. E., Yu, M., Xin, J., Liu, Z., and Wang, Z.: Modeling study of the 2010 regional haze event in the North China Plain, Atmos. Chem. Phys., 16, 1673–1691, doi:10.5194/acp-16-1673-2016, 2016a.

Gao, J., Zhu, B., Xiao, H., Kang, H., Hou, X., and Shao, P.: A case study of surface ozone source apportionment during a high concentration episode, under frequent shifting wind conditions over the Yangtze River Delta, China, Sci. Total Environ., 544, 853, <https://doi.org/10.1016/j.scitotenv.2015.12.039>, 2016b.

Gao, M., Liu, Z., Wang, Y., Lu, X., Ji, D. and Wang, L.: Distinguishing the roles of meteorology, emission control measures, regional transport, and co-benefits of reduced aerosol feedbacks in “APEC” Blue, Atmos. Environ., 167, 476–486, 420 doi:10.1016/j.atmosenv.2017.08.054, 2017.

Gao, Y., Zhang, M., Liu, Z., Wang, L., Wang, P., Xia, X., Tao, M., and Zhu, L.: Modeling the feedback between aerosol and meteorological variables in the atmospheric boundary layer during a severe fog–haze event over the North China Plain, Atmos. Chem. Phys., 15, 4279–4295, doi:10.5194/acp-15-4279-2015, 2015.

Goncalves, M., Jimenez-Guerrero, P., Baldasano, J.M.: Contribution of atmospheric processes affecting the dynamics of air pollution in South-Western Europe during a typical summertime photochemical episode, Atmos. Chem. Phys., 9, 849 – 864, doi:10.5194/acp-9-849-2009, 2009.

- Grell, G. A., Peckham, S. E., Schmitz, R., McKeen, S. A., Frost, G., Skamarock, K., and Eder, B.: Fully coupled “online” chemistry within the WRF model, *Atmos. Environ.*, 39, 6957–6975, 2005.
- Guenther, A., Karl, T., Harley, P., Wiedinmyer, C., Palmer, P. I., and Geron, C.: Estimates of global terrestrial isoprene emissions using MEGAN (Model of Emissions of Gases and Aerosols from Nature), *Atmos. Chem. Phys.*, 6, 3181–3210, doi:10.5194/acp-6-3181-2006, 2006.
- Hansen, J., Sato, M., and Ruedy, R.: Radiative forcing and climate response, *J. Geophys. Res.*, 102, 6831–6864, 1997.
- Haywood, J. and Boucher, O.: Estimates of the direct and indirect radiative forcing due to tropospheric aerosols: A review, *Rev. Geophys.*, 38, 513–543, 2000.
- Hong, S.-Y., Noh, Y., and Dudhia, J.: A New Vertical Diffusion Package with an Explicit Treatment of Entrainment Processes, *Mon. Weather Rev.*, 134, 2318–2341, 2006.
- Iacono, M. J., Delamere, J. S., Mlawer, E. J., Shephard, M. W., Clough, S. A., and Collins, W. D.: Radiative forcing by long-lived greenhouse gases: Calculations with the AER radiative transfer models, *J. Geophys. Res.*, 113, D13103, doi:10.1029/2008JD009944, 2008.
- ~~Jin, X. and Holloway, T.: Spatial and temporal variability of ozone sensitivity over China observed from the Ozone Monitoring Instrument, *J. Geophys. Res. Atmos.*, 120, 7229–7246, <https://doi.org/10.1002/2015JD023250>, 2015.~~
- Li, G., Bei, N., Tie, X., and Molina, L. T.: Aerosol effects on the photochemistry in Mexico City during MCMA-2006/MILAGRO campaign, *Atmos Chem Phys*, 11, 5169–5182, 10.5194/acp-11-5169-2011, 2011.
- Li, J. D., Liao, H., Hu, J. L., Li, N.: Severe particulate pollution days in China during 2013–2018 and the associated typical weather patterns in Beijing–Tianjin–Hebei and the Yangtze River Delta regions, *Environmental Pollution*, 248, 74–81, 2019a.
- Li, K., Jacob, D. J., Liao, H., Zhu, J., Shah, V., Shen, L., Bates, K. H., Zhang, Q., and Zhai, S.: A two-pollutant strategy for improving ozone and particulate air quality in China, *Nat. Geosci.*, 12, 906–910, <https://doi.org/10.1038/s41561-019-0464-x>,

2019<sup>b</sup>.

- Li, M., Zhang, Q., Kurokawa, J.-I., Woo, J.-H., He, K., Lu, Z., Ohara, T., Song, Y., Streets, D. G., Carmichael, G. R., Cheng, Y., Hong, C., Huo, H., Jiang, X., Kang, S., Liu, F., Su, H., and Zheng, B.: MIX: a mosaic Asian anthropogenic emission inventory under the international collaboration framework of the MICS-Asia and HTAP, *Atmos. Chem. Phys.*, 17, 935–963, <https://doi.org/10.5194/acp-17-935-2017>, 2017a.
- Li, Z., Guo, J., Ding, A., Liao, H., Liu, J., Sun, Y., Wang, T., Xue, H., Zhang, H., and Zhu, B.: Aerosol and boundary-layer interactions and impact on air quality, *Nat. Sci. Rev.*, 4, 810–833, <https://doi.org/10.1093/nsr/nwx117>, 2017b.
- Liao, H., Yung, Y. L., and Seinfeld, J. H.: Effects of aerosols on tropospheric photolysis rates in clear and cloudy atmospheres, *J. Geophys. Res.*, 104, 23697–23707, 1999.
- Liao, L., Lou, S. J., Fu, Y., Chang, W. Y., and Liao, H.: Radiative forcing of aerosols and its impact on surface air temperature on the synoptic scale in eastern China [in Chinese], *Chin. J. Atmos. Sci.*, 39, 68–82, doi: 10.3878/j.issn.1006-9895.1402.13302, 2015.
- Lin, Y.-L., Farley, R. D., and Orville, H. D.: Bulk parameterization of the snow field in a cloud model, *J. Clim. Appl. Meteorol.*, 22, 1065–1092, 1983.
- Liu, Y. and Wang, T.: Worsening urban ozone pollution in China from 2013 to 2017 – Part 1: The complex and varying roles of meteorology, *Atmos. Chem. Phys.*, 20, 6305–6321, <https://doi.org/10.5194/acp-20-6305-2020>, 2020.
- Lo, J. C.-F., Yang, Z. L., and Pielke Sr, R. A.: Assessment of three dynamical climate downscaling methods using the Weather Research and Forecasting (WRF) model, *J. Geophys. Res.*, 113, D09112, doi:10.1029/2007jd009216, 2008.
- Lohmann, U., and Feichter, J.: Global indirect aerosol effects: A review. *Atmospheric Chemistry and Physics*, 5, 715–737, <https://doi.org/10.5194/acp-5-715-2005>, 2005.
- Lou, S., Liao, H., and Zhu, B.: Impacts of aerosols on surface-layer ozone concentrations in China through heterogeneous reactions and changes in photolysis rates, *Atmos. Environ.*, 85, 123–138, 2014.
- Miao, Y., Liu, S., Guo, J., Huang, S., Yan, Y., and Lou, M.: Unraveling the

- relationships between boundary layer height and PM<sub>2.5</sub> pollution in China based on four-year radiosonde measurements, *Environmental Pollution*, <https://doi.org/10.1016/j.envpol.2018.09.070>, 2018.
- Otte, T. L.: The impact of nudging in the meteorological model for retrospective air quality simulations. Part I: Evaluation against national observation networks. *J. Appl. Meteor. Climatol.*, 47, 1853–1867, 2008.
- Petäjä, T., Järvi, L., Kerminen, V. M., Ding, A. J., Sun, J. N., Nie, W., Kujansuu, J., Virkkula, A., Yang, X., Fu, C. B., Zilitinkevich, S., and Kulmala, M.: Enhanced air pollution via aerosol-boundary layer feedback in China, *Sci. Rep.*, 6, 18998, doi:10.1038/srep18998, 2016.
- Qiu, Y., Liao, H., Zhang, R., and Hu, J.: Simulated impacts of direct radiative effects of scattering and absorbing aerosols on surface layer aerosol concentrations in China during a heavily polluted event in February 2014, *J. Geophys. Res. Atmos.*, 122, 5955–5975, doi:10.1002/2016JD026309, 2017.
- Skamarock, W., Klemp, J. B., Dudhia, J., Gill, D. O., Barker, D. M., Duda, M., Huang, X. Y., Wang, W., and Powers, J. G.: A description of the advanced research WRF version 3, NCAR technical note NCAR/TN/u2013475, 2008.
- Tang, G. Q., Zhu, X. W., Xin, J. Y., Hu, B., Song, T., Sun, Y., Zhang, J. Q., Wang, L. L., Cheng, M. T., Chao, N., Kong, L. B., Li, X., and Wang, Y. S.: Modelling study of boundary-layer ozone over northern China – Part I: Ozone budget in summer, *Atmos. Res.*, 187, 128–137, 2017.
- ~~Tang, G., Zhang, J., Zhu, X., Song, T., Munkel, C., Hu, B., Schäfer, K., Liu, Z., Zhang, J., Wang, L., Xin, J., Suppan, P., and Wang, Y.: Mixing layer height and its implications for air pollution over Beijing, China, *Atmos. Chem. Phys.*, 16, 2459–2475, doi:10.5194/acp-16-2459-2016, 2016.~~
- Tie, X., Geng, F., Li, P., Gao, W., and Zhao, C.: Measurement and modelling of ozone variability in Shanghai, China, *Atmos. Environ.*, 43, 4289–4302, 2009.
- Wang, W., Li, X., Shao, M., Hu, M., Zeng, L., Wu, Y., and Tan, T.: The impact of aerosols on photolysis frequencies and ozone production in Beijing during the 4-year period 2012–2015, *Atmos. Chem. Phys.*, 19, 9413–9429,

<https://doi.org/10.5194/acp19-9413-2019>, 2019.

Wild, O., Zhu, X., and Prather, M. J.: Fast-J: Accurate simulation of in- and below-cloud photolysis in tropospheric chemical models, *J. Atmos. Chem.*, 37, 245–282, doi:10.1023/A:1006415919030, 2000.

Wu, J., Bei, N., Hu, B., Liu, S., Wang, Y., Shen, Z., Li, X., Liu, L., Wang, R., Liu, Z., Cao, J., Tie, X., Molina, L. T., Li, G.: Aerosol-photolysis interaction reduces particulate matter during wintertime haze events, *Proc. Natl. Acad. Sci. USA*, 117, 9755–9761, 2020.

Xing, J., Wang, J. D., Mathur, R., Wang, S. X., Sarwar, G., Pleim, J., Hogrefe, C., Zhang, Y. Q., Jiang, J. K., Wong, D. and Hao, J. M.: Impacts of aerosol direct effects on tropospheric ozone through changes in atmospheric dynamics and photolysis rates, *Atmos. Chem. Phys.*, 17, 9869–9883, <https://doi.org/10.5194/acp-17-9869-2017>, 2017.

Zaveri, R. A. and Peters, L. K.: A new lumped structure photochemical mechanism for large-scale applications, *J. Geophys. Res.*, 104, D23, 30387–30415, <https://doi.org/10.1029/1999JD900876>, 1999.

Zaveri, R. A., Easter, R. C., Fast, J. D., and Peters, L. K.: Model for simulating aerosol interactions and chemistry (MOSAIC), *J. Geophys. Res.*, 113, D13204, <https://doi.org/10.1029/2007JD008782>, 2008.

Zhang, X., Zhang, Q., Hong, C. P., Zheng, Y. X., Geng, G. N., Tong, D., Zhang, Y. X., and Zhang, X. Y.: Enhancement of PM<sub>2.5</sub> concentrations by aerosol-meteorology interactions over China. *Journal of Geophysical Research: Atmospheres*, 123, 1179–1194, <https://doi.org/10.1002/2017JD027524>, 2018.

Zhang, Y., Wen, X.-Y., and Jang, C. J.: Simulating chemistry–aerosol–cloud–radiation–climate feedbacks over the continental US using the online-coupled Weather Research Forecasting Model with chemistry (WRF/Chem), *Atmos. Environ.*, 44, 3568–3582, doi:10.1016/j.atmosenv.2010.05.056, 2010.

Zhao, H.; Zheng, Y., and Li, C. Spatiotemporal distribution of PM<sub>2.5</sub> and O<sub>3</sub> and their interaction during the summer and winter seasons in Beijing, China. *Sustainability*, 10, 4519, 2018.

673 Zhou, M., Zhang, L., Chen, D., Gu, Y., Fu, T.-M., Gao, M., Zhao, Y., Lu, X. and Zhao,  
674 B.: The impact of aerosol-radiation interactions on the effectiveness of emission  
675 control measures, Environmental Research Letters, 14(2), 024002,  
676 <https://doi.org/10.1088/1748-9326/aaf27d>, 2019.

677 Zhu, J., Chen, L., Liao, H., and Dang, R.: Correlations between PM<sub>2.5</sub> and Ozone over  
678 China and Associated Underlying Reasons, Atmosphere, 352, 1–15,  
679 <https://doi.org/10.3390/atmos10070352>, 2019.

680 Zhu, J., Chen, L., Liao, H., Yang, H., Yang, Y., and Yue, X.: Enhanced PM<sub>2.5</sub> Decreases  
681 and O<sub>3</sub> Increases in China During COVID-19 Lockdown by Aerosol-Radiation  
682 Feedback, Geophys. Res. Lett., 48, <https://doi.org/10.1029/2020GL090260>, 2021.

1 **Table 1.** Physical parameterization options used in the simulation.

Options	Schemes
<b>Microphysics scheme</b>	Lin (Purdue) scheme (Lin et al.,1983)
<b>Cumulus scheme</b>	Grell 3D ensemble scheme
<b>Boundary layer scheme</b>	Yonsei University PBL scheme (Hong et al., 2006)
<b>Surface layer scheme</b>	Monin-Obukhov surface scheme (Foken, 2006)
<b>Land-surface scheme</b>	Unified Noah land-surface model (Chen and Dudhia, 2001)
<b>Longwave radiation scheme</b>	RRTMG (Iacono et al., 2008)
<b>Shortwave radiation scheme</b>	RRTMG (Iacono et al., 2008)

2

**Table 2.** Statistical parameters between simulated and observed PM<sub>2.5</sub> (μg m<sup>-3</sup>), O<sub>3</sub> (ppb), 2-m temperature (T<sub>2</sub>, °C), 2-m relative humidity (RH<sub>2</sub>, %), 10-m wind speed (WS<sub>10</sub>, m s<sup>-1</sup>), and photolysis rate of NO<sub>2</sub> (J[NO<sub>2</sub>], s<sup>-1</sup>) during 28 July to 3 August 2014.

Variables	$\bar{O}^a$	$\bar{M}^a$	$R^b$	$MB^c$	$ME^d$	$NMB^e(\%)$	$NME^f(\%)$	$RMSE^g$
PM <sub>2.5</sub>	113.3	90.7	0.66	-21.8	25.2	-19.2	22.2	30.1
O <sub>3</sub>	47.7	44.1	0.86	-5.7	15.5	-12.0	32.4	18.2
T <sub>2</sub>	28.4	28.0	0.98	-0.2	0.9	-0.7	3.3	1.1
RH <sub>2</sub>	70.9	65.7	0.93	-6.0	6.7	-8.5	9.5	8.7
WS <sub>10</sub>	2.4	3.0	0.70	0.6	0.9	27.9	36.6	1.0
J[NO <sub>2</sub> ]	1.6×10 <sup>-3</sup>	1.8×10 <sup>-3</sup>	0.97	1.1×10 <sup>-4</sup>	3×10 <sup>-4</sup>	6.8	18.5	5.3×10 <sup>-4</sup>

<sup>a</sup> $\bar{O}$  and  $\bar{M}$  are the averages for observed and simulated results, respectively.  $\bar{O} =$

$$\frac{1}{n} \times \sum_{i=1}^n O_i, \bar{M} = \frac{1}{n} \times \sum_{i=1}^n M_i.$$

<sup>b</sup> $R$  is the correlation coefficient between observations and model results.  $R =$

$$\frac{\sum_{i=1}^n |(O_i - \bar{O}) \times (M_i - \bar{M})|}{\sqrt{\sum_{i=1}^n (O_i - \bar{O})^2 \times \sum_{i=1}^n (M_i - \bar{M})^2}}.$$

<sup>c</sup> $MB$  is the mean bias between observations and model results.  $MB = \frac{1}{n} \times \sum_{i=1}^n (M_i - O_i).$

<sup>d</sup> $ME$  is the mean error between observations and model results.  $ME = \frac{1}{n} \times \sum_{i=1}^n |M_i - O_i|.$

<sup>e</sup> $NMB$  is the normalized mean bias between observations and model results.  $NMB =$

$$\frac{1}{n} \times \sum_{i=1}^n \frac{M_i - O_i}{O_i} \times 100\%.$$

<sup>f</sup> $NME$  is normal mean error between observations and model results.  $NME =$

$$\frac{1}{n} \times \sum_{i=1}^n \frac{|M_i - O_i|}{O_i} \times 100\%.$$

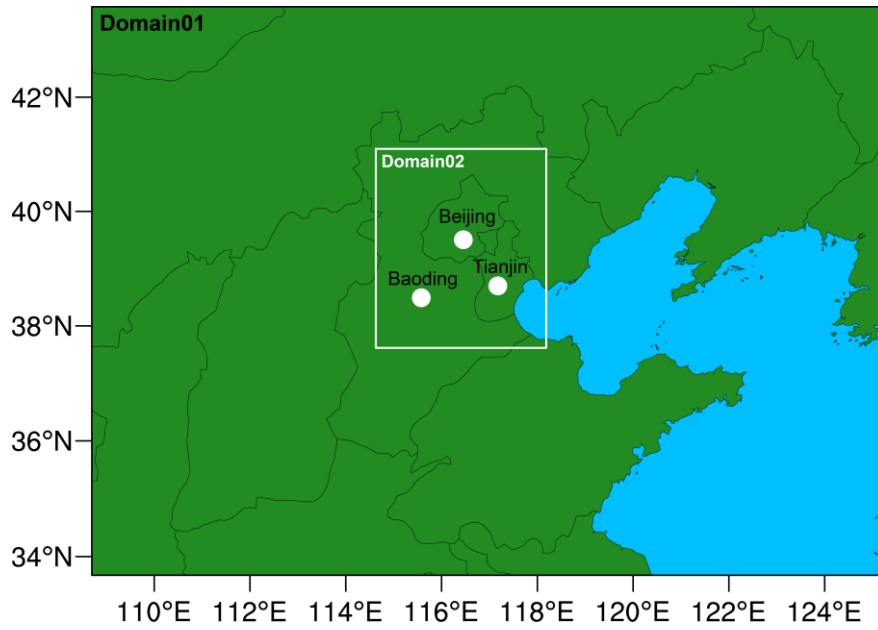
<sup>g</sup> $RMSE$  is the root mean square error of observations and model results.  $RMSE =$

$$\sqrt{\frac{1}{n} \times \sum_{i=1}^n (M_i - O_i)^2}.$$

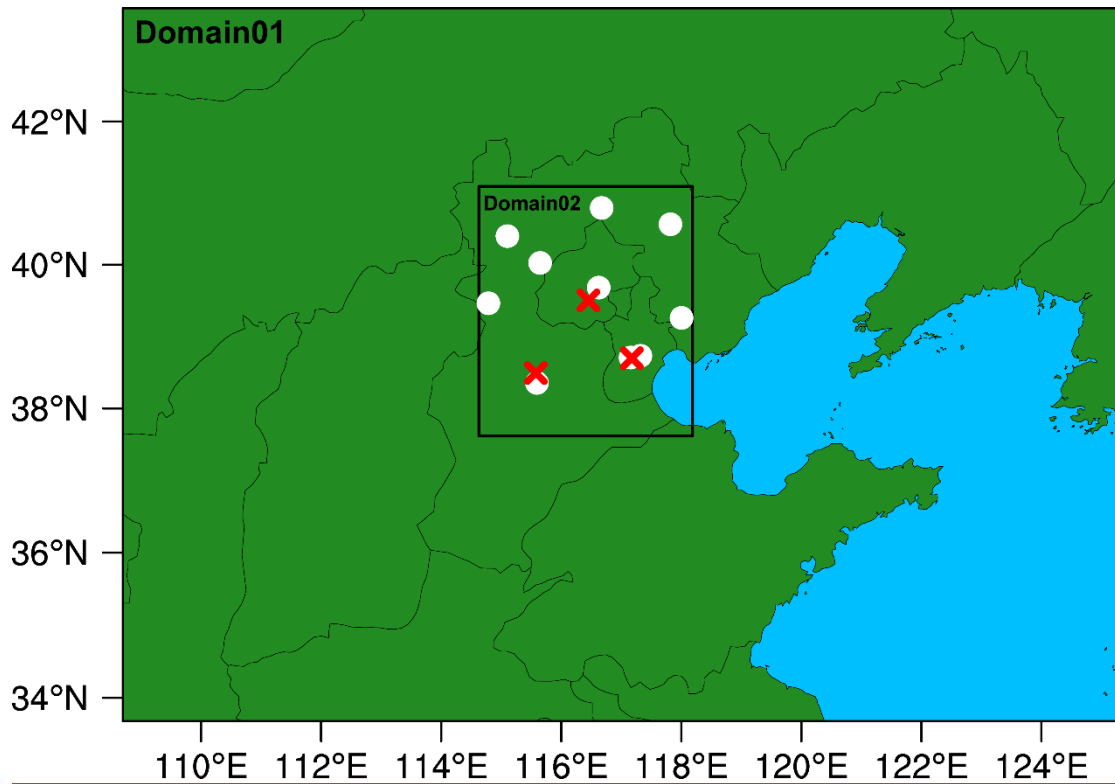
In the above  $O_i$  and  $M_i$  are the hourly observed and simulated data, respectively, and  $n$  is the total number of hours.



1



2



3 **Figure 1.** Map of the two WRF-Chem modeling domains with the locations of  
 4 meteorological (white dots) and environmental (red crosses) observation sites used for  
 5 model evaluation.~~Map of the two WRF-Chem modeling domains and the locations of~~  
 6 ~~observation sites (white dots) used for model evaluation.~~  
 7

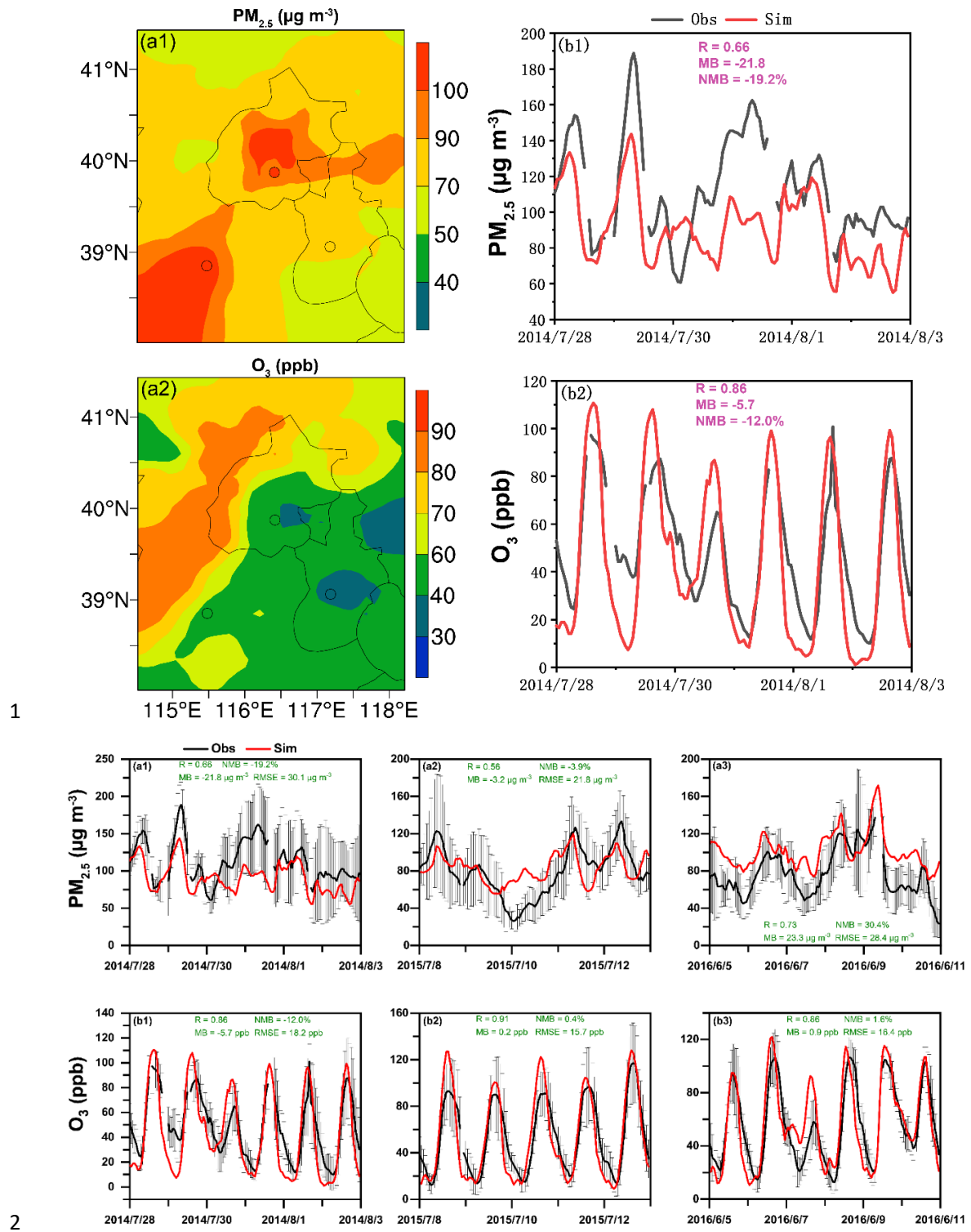


**Figure 2.** Time series of observed (black) and simulated (red) hourly surface (a)  $PM_{2.5}$  and (b)  $O_3$  concentrations averaged over the thirty-two observation sites in Beijing, Tianjin, and Baoding during 28 July to 3 August 2014 (Episode1, a1-b1), 8-13 July 2015 (Episode2, a2-b2) and 5-11 June 2016 (Episode3, a3-b3). The error bars represent the standard deviations. The calculated correlation coefficient (R), mean bias (MB), normalized mean bias (NMB) and root-mean-square error (RMSE) are also shown. (a1-a2) Spatial distributions of simulated (color counters) and observed (colored circles)

1 ~~PM<sub>2.5</sub> and O<sub>3</sub> concentrations averaged during 28 July to 3 August 2014. (b1 b2) Time~~  
2 ~~series of observed (black) and simulated (red) hourly PM<sub>2.5</sub> and O<sub>3</sub> concentrations~~  
3 ~~averaged over the 32 observation sites in Beijing, Tianjin, and Baoding. The calculated~~  
4 ~~correlation coefficient (R), mean bias (MB), and normalized mean bias (NMB) are also~~  
5 ~~shown.~~

6

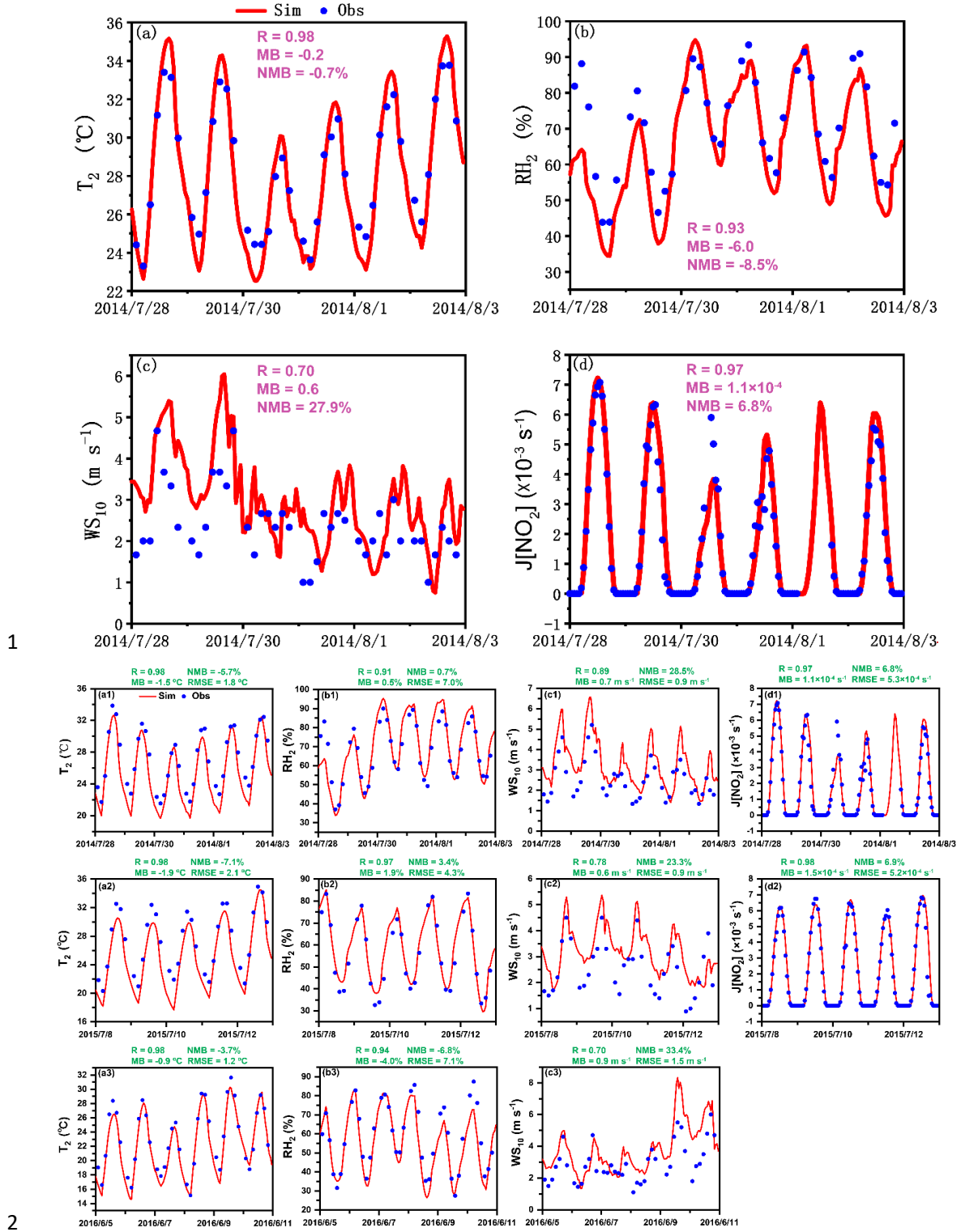
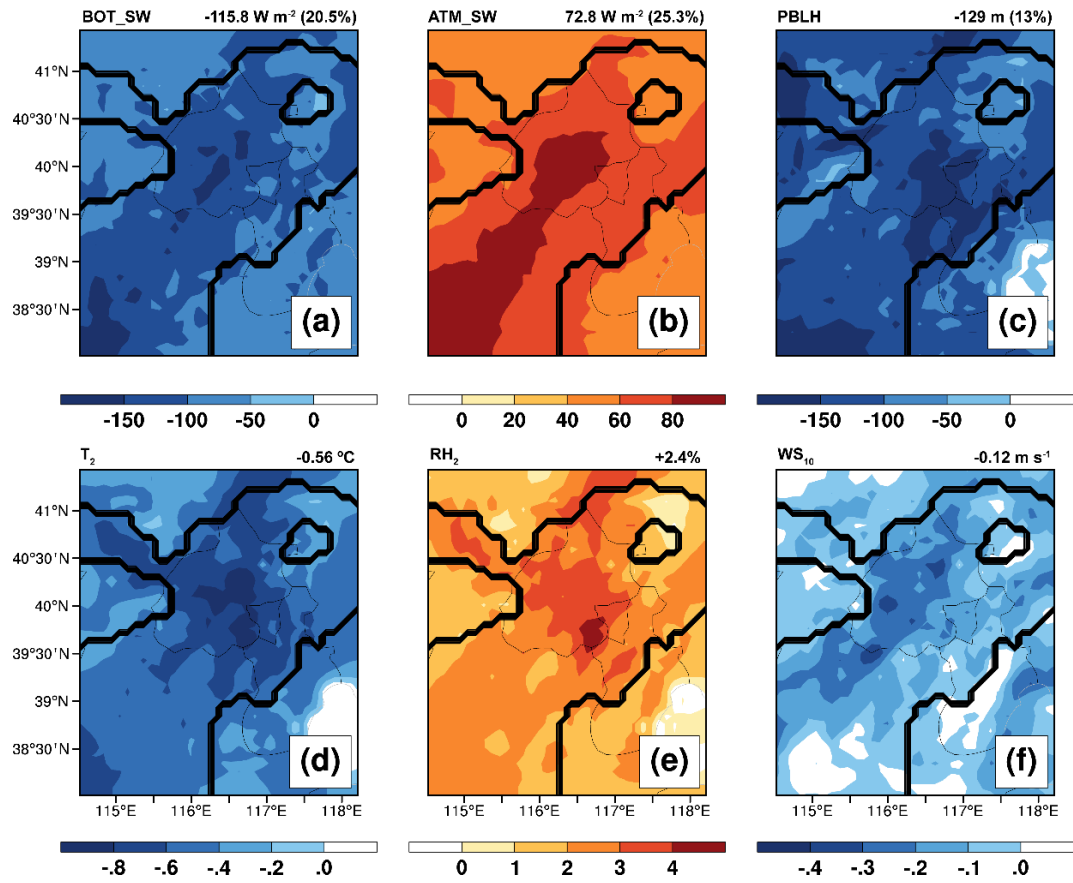


**Figure 3.** Time series of 3-hourly observed (blue dots) and hourly simulated (red lines) (a) 2-m temperature ( $T_2$ ), (b) 2-m relative humidity ( $RH_2$ ), (c) wind speed at 10 m ( $WS_{10}$ ) averaged over ten meteorological observation stations, and (d) surface photolysis rate of  $NO_2$  ( $J[NO_2]$ ) during 28 July to 3 August 2014 (Episode1, a1-d1), 8-13 July 2015 (Episode2, a2-d2) and 5-11 June 2016 (Episode3, a3-c3). The calculated correlation coefficient ( $R$ ), mean bias ( $MB$ ), and normalized mean bias ( $NMB$ ) and root-mean-square error ( $RMSE$ ) are also shown.



1

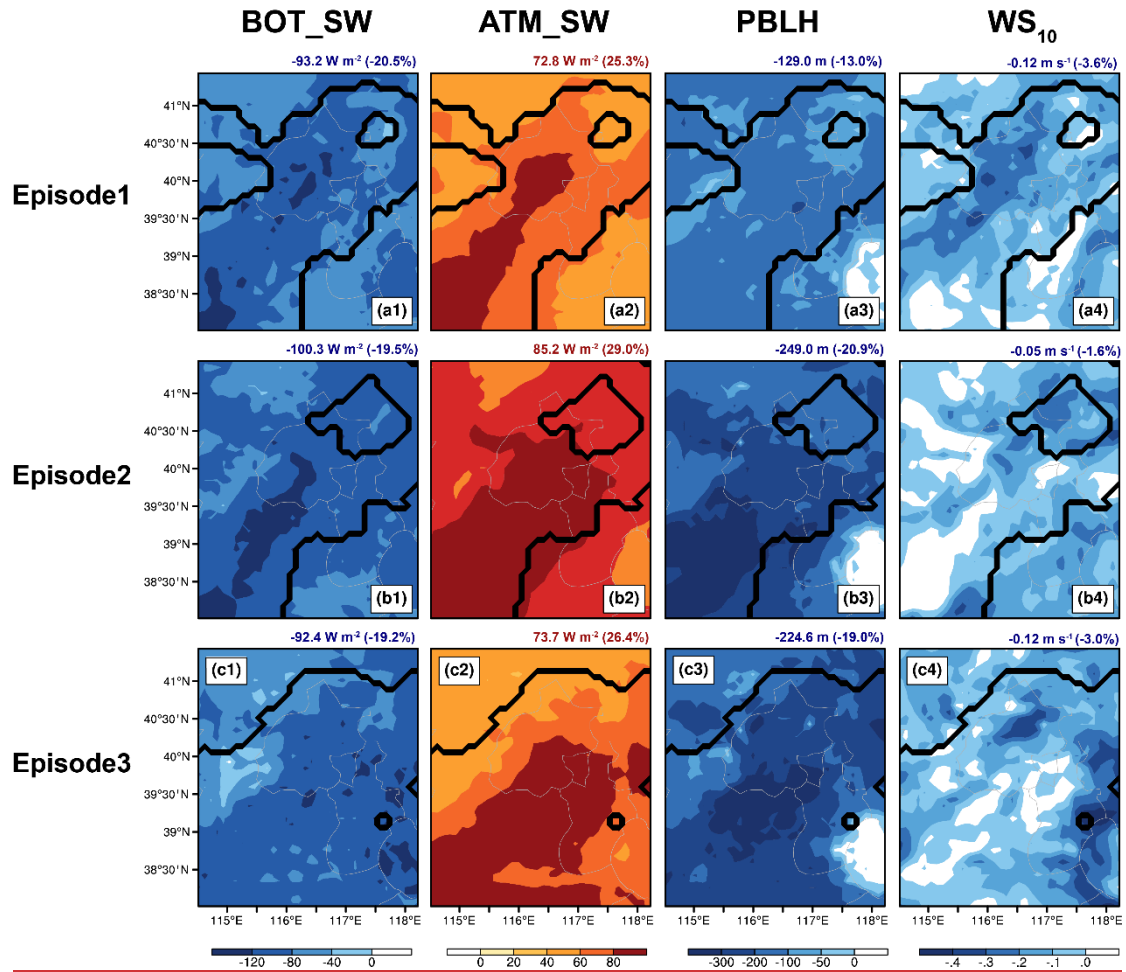
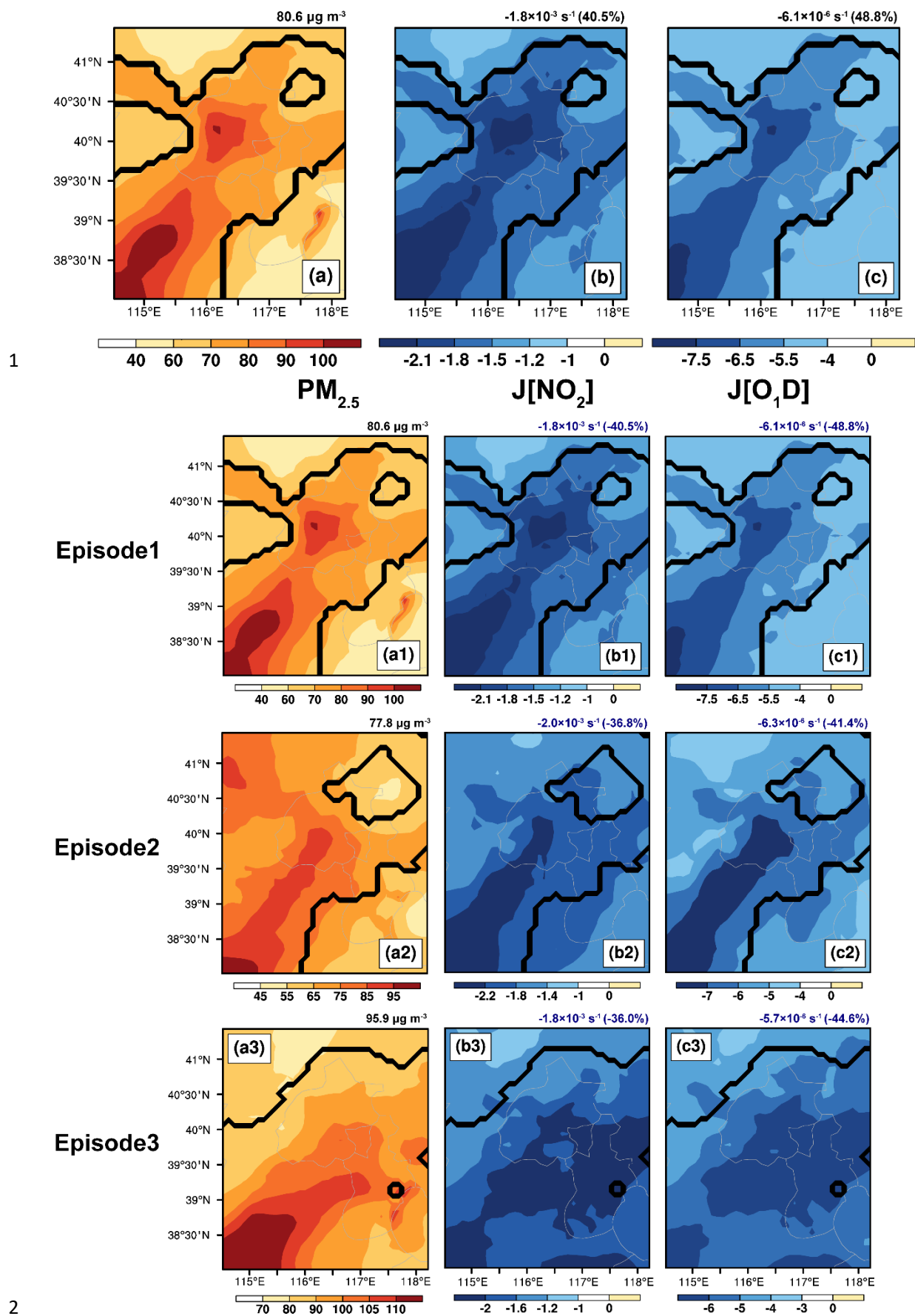
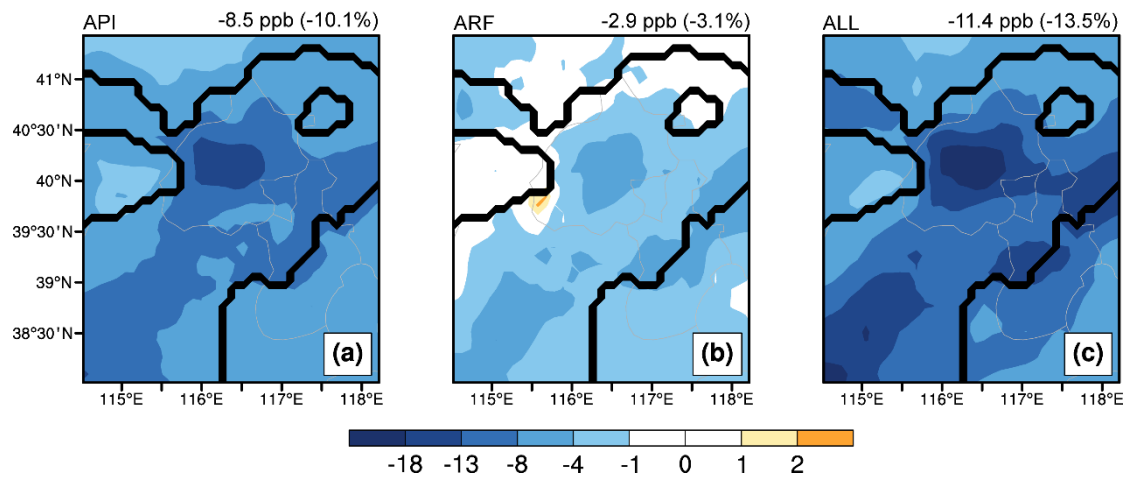


**Figure 4.** The impacts of aerosol-radiation interactions on (a) downward-shortwave radiation at the surface (BOT\_SW), (b) downward-shortwave radiation in the atmosphere (ATM\_SW), (c) PBL height (PBLH), (d) 2-m temperature ( $T_2$ ), (e) 2-m relative humidity ( $RH_2$ ), and (f) 10-m wind speed ( $WS_{10}$ ) during in the daytime (08:00-17:00 LST) during from 28 July to 3 August 2014 (Episode1), 8-13 July 2015 (Episode2) and 5-11 June 2016 (Episode3). The regions sandwiched between two black lines is are defined as the complex air pollution areas (CAPAs) where the mean daily  $PM_{2.5}$  and MDA8  $O_3$  concentrations in BASE case are larger than  $75 \mu\text{g m}^{-3}$  and 80 ppb. The calculated changes (percentage changes) averaged over CAPAs are also shown shown at the top of each panel.



1 BASE cases, and the changes in surface (b) J[NO<sub>2</sub>] and (c) J[O<sup>1</sup>D] due to aerosol-  
2 radiation interactions ~~during-in~~ the daytime (08:00-17:00 LST) during 28 July to 3  
3 August 2014 (Episode1), 8-13 July 2015 (Episode2) and 5-11 June 2016  
4 (Episode3)~~from 28 July to 3 August 2014~~. The calculated values (percentage changes)  
5 averaged over CAPAs are also ~~shwon~~shown at the top of each panel.





1

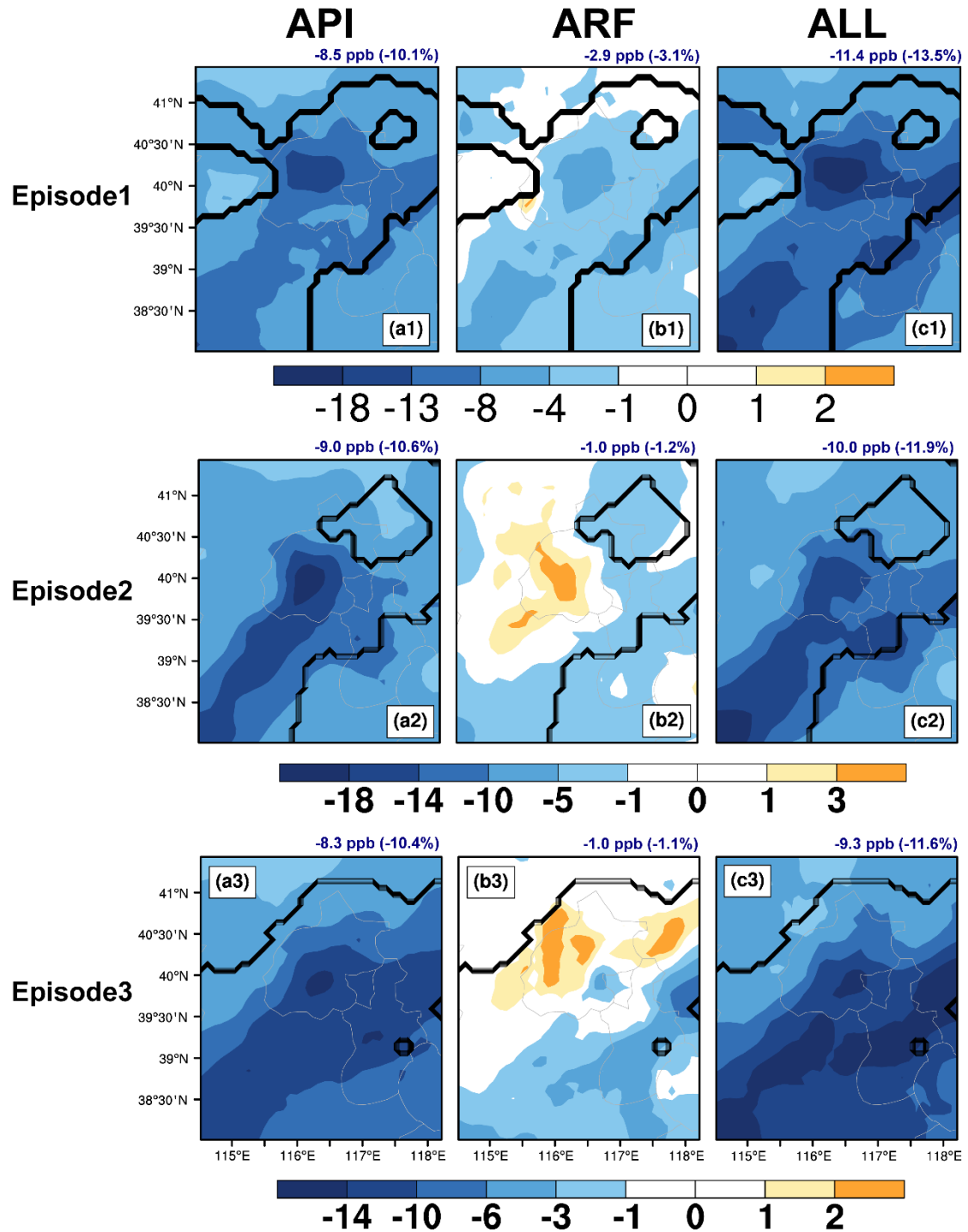


**Figure 6.** The changes in surface-layer ozone due to (a) aerosol-photolysis interaction (API), (b) aerosol-radiation feedback (ARF), and (c) the combined effects (ALL, defined as API+ARF) during-in the daytime (08:00-17:00 LST) during 28 July to 3 August 2014 (Episode1), 8-13 July 2015 (Episode2) and 5-11 June 2016 (Episode3)from 28 July to 3 August 2014. The calculated mean changes (percentage changes) avaraged over CAPAs are also shown at the top of each panel.

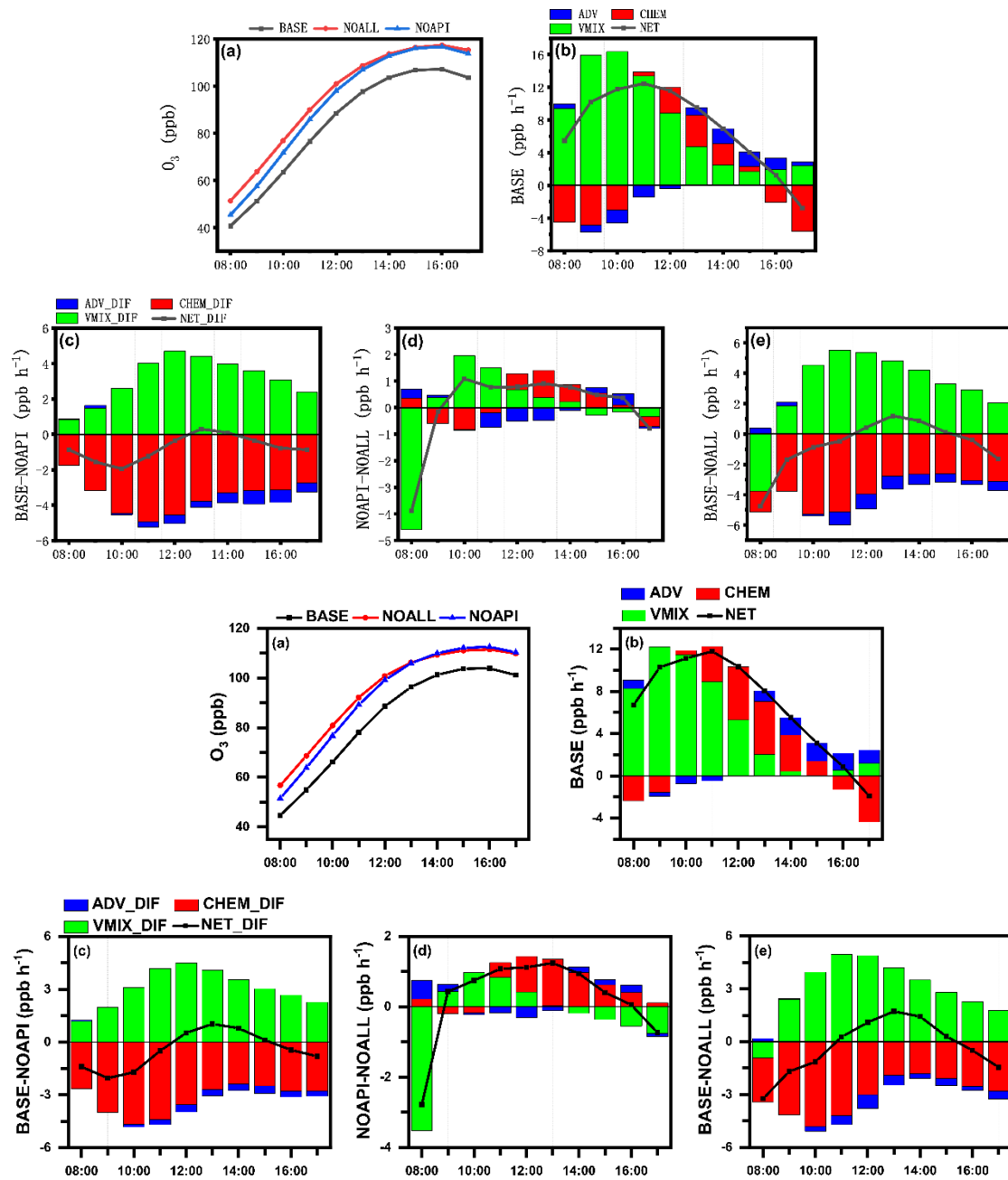
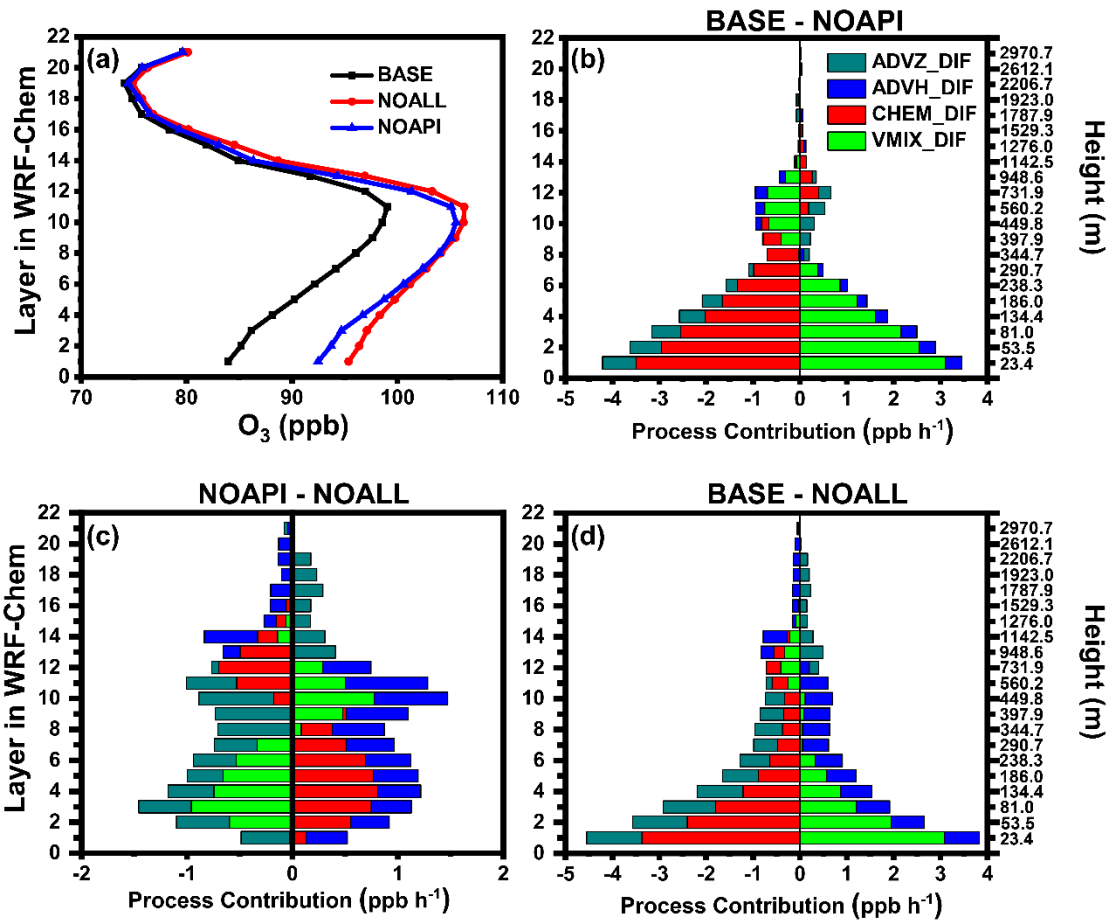


**Figure 7. Temporal evolution characteristics of aerosol-radiation interactions on  $O_3$  averaged over the three episodes.** (a) Diurnal variations of simulated  $O_3$  concentrations in BASE (black dotted line), NOAPI (blue dotted line), and NOALL (red dotted line) cases over CAPAs. (b) The hourly  $O_3$  changes induced by each physical/chemical process using the IPR analysis method in BASE case. (c-e) Changes in hourly  $O_3$  process contributions caused by API (BASE minus NOAPI), ARF (NOAPI minus NOALL), and ALL (BASE minus NOALL) over CAPAs during the daytime (08:00-17:00 LST) from 28 July to 3 August 2014. The black lines with squares denote the net contribution of all processes (NET, defined as VMIX+CHEM+ADV). Differences of each process contribution are denoted as VMIX\_DIF, CHEM\_DIF, ADV\_DIF, and NET\_DIF.



1

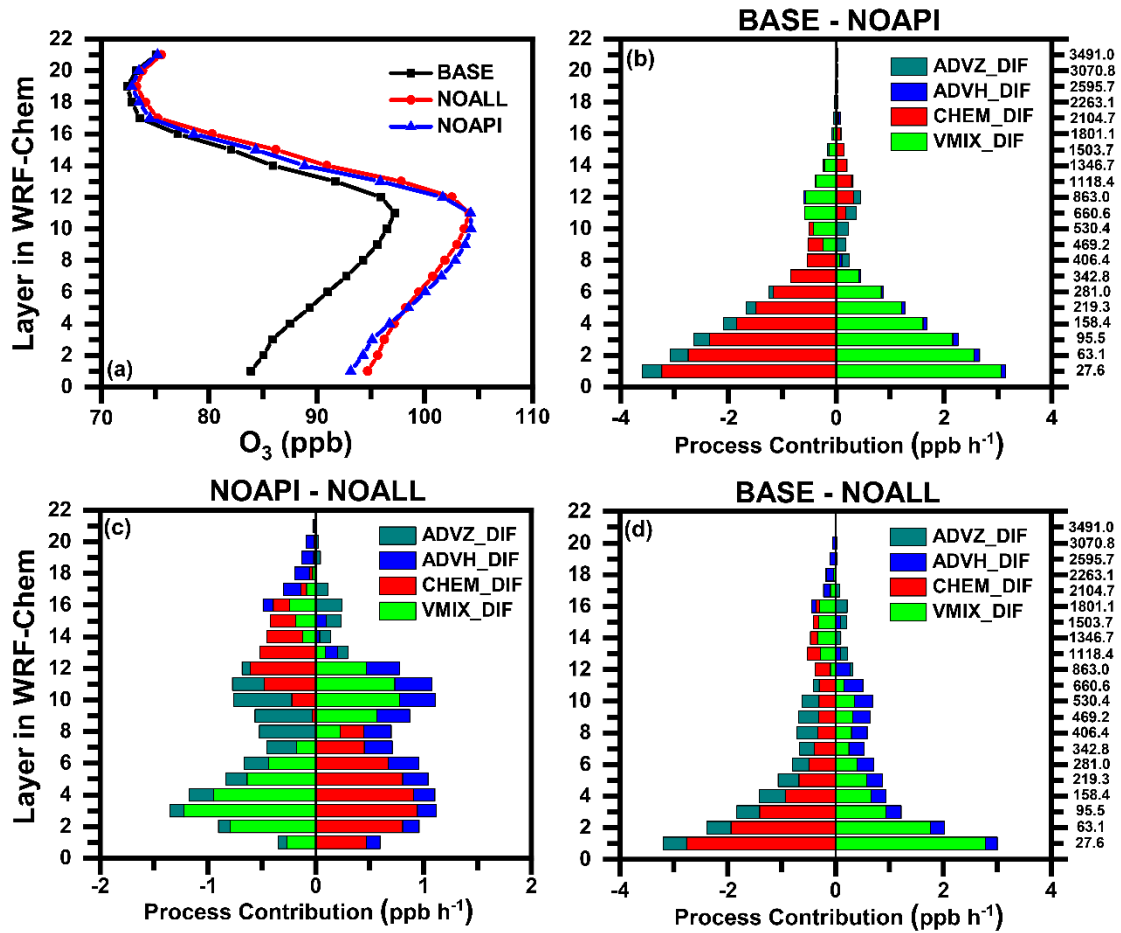


**Figure 8.** The impacts of aerosol-radiation interactions on vertical  $O_3$  averaged over the three episodes. (a) Vertical profiles of simulated  $O_3$  concentrations in BASE (black dotted line), NOAPI (blue dotted line), and NOALL (red dotted line) cases over CAPAs. (b-d) Changes in  $O_3$  budget due to API, ARF, and ALL over CAPAs during the daytime (08:00-17:00 LST) ~~from 28 July to 3 August 2014~~. Differences of each process contribution are denoted by ADVZ\_DIF, ADVH\_DIF, CHEM\_DIF, and VMIX\_DIF.